IEEE Access
Multidisciplinary | Rapid Review | Open Access Journal

Received April 17, 2020, accepted April 28, 2020, date of publication May 6, 2020, date of current version May 20, 2020.

Digital Object Identifier 10.1109/ACCESS.2020.2992660

NOMA in Cooperative Underlay Cognitive Radio Networks Under Imperfect SIC

DINH-THUAN DO[1], (Senior Member, IEEE), ANH-TU LE[2], AND BYUNG MOO LEE[3], (Member, IEEE)

[1]Wireless Communications Research Group, Faculty of Electrical and Electronics Engineering, Ton Duc Thang University, Ho Chi Minh City 758307, Vietnam
[2]Faculty of Electronics Technology, Industrial University of Ho Chi Minh City, Ho Chi Minh City 71406, Vietnam
[3]School of Intelligent Mechatronics Engineering, Sejong University, Seoul 05006, South Korea

Corresponding authors: Dinh-Thuan Do (dodinhthuan@tdtu.edu.vn) and Byung Moo Lee (blee@sejong.ac.kr)

This work was supported by the Basic Science Research Program through the National Research Foundation of Korea (NRF) funded by the Korea government, Korea Government under Grant NRF-2019R1A4A1023746 and Grant NRF-2017R1D1A1B03028350.

ABSTRACT In conventional cognitive radio (CR), the users in secondary network (SN) can only access the idle spectrum when users in primary network (PN) are absent. This novel strategy provides higher spectrum efficiency when detecting the presence of the PN. Hence, spectrum utilization of the traditional scheme can be further improved as exploiting application of non-orthogonal multiple access (NOMA). As combination of CR and NOMA, such CR-NOMA has been proposed to improve spectrum efficiency to adapt to requirements in 5G communications. In this study, the relaying scheme is employed in the SN of the proposed CR-NOMA and the relay is allowed to energy harvesting (EH) from the secondary transmitter to serve signal forwarding to distant secondary users. With this regard, the complex model of EH-assisted CR-NOMA is explored in outage behavior and throughput performance as awareness on imperfect successive interference cancellation (SIC) at the receiver. As most important results, the exact closed-form of the exact outage probability is derived for each NOMA destination by assuming that the channel coefficients among considered links follow Rayleigh distribution. Furthermore, performance gap between two NOMA users can be controlled by various parameters such as transmit power, energy harvesting coefficients and levels of imperfect SIC. Simulation results verify our analytical results.

INDEX TERMS Energy harvesting, imperfect SIC, NOMA, outage probability, underlay cognitive radio.

I. INTRODUCTION

Considering as a candidate for the fifth generation (5G) wireless communication, a novel multiple access (MA) technique is recently required to investigate, namely non-orthogonal multiple access (NOMA). Comparing with the fourth generation (4G) systems, 5G systems will not be considered as its incremental version, future wireless systems have anticipated functionality, such as cloud-based applications and internet-of-things (IoT). To adapt to these challenges, several requirements are considered, such as higher data rates, low latency, massive connectivity, higher spectral and power efficiency. For example, NOMA is proposed and widely conducted due to its characteristics such as superior spectral efficiency, balanced user fairness, intense connections and low access latency [1]–[5]. In addition, the non-orthogonal resource allocation is explored in NOMA to implement emerging networks such as satellite hybrid relaying network, unmanned aerial vehicle [6]. The challenging models are developed by the authors in [7]–[9], in which combination between relay schemes and NOMA is introduced as novel scheme, namely cooperative NOMA. The novel idea of NOMA is to divide the power domain for realizing multiple access (MA). In NOMA, different power levels are allocated for different users with respect to distinguished signals [10], [11]. Depending on channel conditions, base station differentiates power to users. In particular, users with poor channel conditions (weak users) are allocated higher power percentage than strong users which occupy better channel conditions. To deploy NOMA, the base station superimposes the multiple information messages to serve many destinations by exploiting superposition coding (SC) scheme. By deployment

The associate editor coordinating the review of this manuscript and approving it for publication was Agustin Leobardo Herrera-May.

of successive interference cancellation (SIC), each NOMA user detects all weaker users' signals by determining stronger users' messages as a noise before decoding the own message [12].

A. RELATED WORKS

In addition, the explosive increment of diverse mobile devices and the rapid development of high-rate services, it is required to explore new paradigms to provide higher spectral efficient and energy-efficient communication networks. However, to attain a high spectral efficiency (SE) the fixed spectrum allocation scheme meets a major disadvantage. Recently, cognitive radio (CR) network has been introduced to allow the primary network to share its frequency band with the secondary network with respect to improved SE [13]. Besides SE, other increasing attention is that energy efficiency (EE), especially in both energy constraint devices and wireless powered systems [14]. In energy-efficient architecture, there are two kinds of energy aware systems. The first kind considers on maximizing EE [15]. In [16], a novel NOMA system was investigated in term of EE power allocation. In particular, they examined a low-complexity sub optimal algorithm which comprises power allocation and sub channel assignment. The second kind is energy harvesting (EH). Recently, radio-frequency (RF) signals have been proposed as promising sources for EH. The EE of the wireless communication networks can be enhanced by examining RF-based EH technique as [17] and [18]. Moreover, information transmission and EH are joint processed due to the dual properties of RF, the authors in [19]–[23] investigated a developing technique, namely simultaneous wireless information and power transfer (SWIPT).

Regarding improved SE, CR-inspired NOMA (CR-NOMA) and NOMA with fixed power allocation are analyzed under several circumstances to prove that channel quality of a user with a poor channel condition could strictly guarantee in the CR-NOMA [24]. In addition, the better fairness in term of spectrum allocation can be obtained in CR-NOMA compared NOMA with the fixed power allocation. In addition, the power allocation is presented for two secondary user to improve the SE in the underlay CR-NOMA by using interference cancellation technique [25]. Thus, to greatly improve the spectrum utilization it is natural to employ NOMA together with CR with power constraints. Furthermore, a large-scale underlay CR system is developed by using stochastic geometry along with NOMA. They derived expressions of the outage probability for the NOMA users to evaluate the performance of the considered networks [26]. Regarding improved EE, joint SWIPT and NOMA was introduced to encourage strong users to forward weak users' signal and then this dual-hop transmission will not drain their batteries [27], [28]. To increase the individual data rate, wireless powered communication networks (WPCN) is proposed to combine with NOMA uplink as [29]. Benefiting from the harvested energy in the first time slot, the strong users in [30] are able to forward to the weak users' signals in the second time slot employing beamforming in half-duplex (HD) manner. The other problem of maximising the data rate is performed for the strong user to satisfy the QoS of the weak user in SWIPT NOMA system at HD mode [31]. The formulated system performance problem need be solved with respect to satisfy both SE and EE requirements and the SWIPT is further jointly implemented. Of course, working in SWIPT NOMA system model in these systems isn't well addressed since interference constraint environment in CR has not been fully considered.

The extra benefits of CR-NOMA networks can be seen as deploying cooperative protocol in such NOMA [32]–[35]. In [32], primary and secondary users are able to receive unicast and multicast information by using NOMA respectively. In this scheme, to access to the primary spectrum the cooperation in the secondary network (SN) is required in such NOMA application. In addition, to enhance the secondary user fairness a two-stage cooperative strategy was investigated in a cooperative multicast CR-NOMA scheme as [33]. The exact expressions are derived to evaluate performance of two NOMA secondary destination users in term of outage probability [34]. They considered worse case as imperfect channel state information occurred and optimal power allocation coefficients can be found as examining different distances to adapt to the outage probability fairness for two users [34].

In other scenario, imperfect SIC is studied by introducing asymptotic expressions related to derived outage probabilities in two situations including when the interference constraint be infinity and when the transmit powers at some nodes be infinity [35]. In other context of NOMA, the strong primary user (PU) communicates confidential signal with multiple uniformly distributed PUs as external eavesdroppers are randomly located and they provided tractable formula to analyze the security and the reliability performance [36]. By exploiting the practical non-linear EH scheme from the RF signals, the secondary users are be able to harvest energy to securely transmit the secondary privacy information [37]. The authors in [38] presented distributed sequential coalition formation (DSCF) paradigm to solve the user grouping problem, where the primary user's spectrum band can be shared with multiple cognitive users within a group while achieving requirement of the primary user with respect to a minimum rate. In recent work [39], CR-NOMA network is deployed channels with capable of independent but necessarily identical distributed Nakagami-*m* fading channels and accurate closed-form analytical expressions are studied to highlight outage probability performance of two secondary NOMA users.

B. OUR CONTRIBUTIONS

In recent research, the authors in [24] derived exact closed-form expressions for CR-NOMA system over Rayleigh fading channels and they targeted their analysis to evaluate outage performance of each secondary destination. However, it need be extended to general framework for such CR-NOMA considering Nakagami-*m* fading channels and limited

power source occurs at the relay in practice. To fill the aforementioned gap, we emphasize on the outage and throughput performance of a CR-NOMA to implement in green communication by introducing wireless power transfer technique. Although CR-NOMA networks are studied as recent research [32], [33], however it is necessary to study a general frame work of CR-NOMA over Nakagami-*m* fading. Unlike recent work [39], they studied a cooperative underlay decode-and-forward (DF) CR-NOMA networks with several assumptions at the secondary relay without EH, perfect SIC and imposed interference temperature constraint. In this study, main goal is that system performance need be evaluated as exploiting how EH-assisted relay remains performance of destination users. Such challenge for EH-assisted relay need be studied since relay does not have individual power due to difficulty in wiring of power grid to its location. The main contributions of this study is summarized as follows:

1) Different with [25], a CR-NOMA is studied to permit secondary network containing the secondary source intends to access the 5G spectrum to serve distant users over Nakagami-*m* fading and Rayleigh fading as well. In particular, secondary source employs NOMA to communicate with two destinations through wireless powered relay. Such CR-NOMA is expected to improve the spectrum utilization greatly compared with the traditional OMA scheme.
2) Impacts of EH parameters on system evaluation have not been well studied in [24], [34], [35]. We first propose two policies of wireless power transfer applied in secondary network to introduce EH-assisted CR-NOMA system. In such system, by reusing harvested energy it can be further improved energy efficiency with respect to serve distant users. Moreover, we also consider impact of the imperfect SIC to signal detecting on the receivers of CR-NOMA in practical applications.
3) We derive the closed-form expressions of the outage probability for two users. Under the high complexity in computation, it is necessary to explore asymptotic outage performance of each user to provide insight for such EH-assisted CR-NOMA. In addition, we examine two scenarios of optimal outage performance as considering how time/power splitting coefficients in EH protocol affect on system performance. Although it is difficult to obtain the closed-form expressions of optimal time/power splitting coefficients, however numerical method is enabled to tackle such optimization problem.
4) Simulation results show the performance comparison in various scenarios of the proposed scheme in terms of the outage probability and throughput, which show slightly different as comparison between time switching relaying (TS) and power splitting relaying (PS) EH model.

The remainder of this paper is organized as follows. Section II defines the system and channel model with a definition of two EH protocols adopted in power constrained relay in such CR-NOMA. Section III consider CR-NOMA system over Rayleigh fading and derives expressions of outage probability for two users. To evaluate the insight performance, asymptotic outage behavior and throughput are further studied. The scenario of Nakagami-*m* fading adopted in CR-NOMA is presented in Section IV. Numerical results are presented in Section V. Finally, the paper is concluded in Section VI.

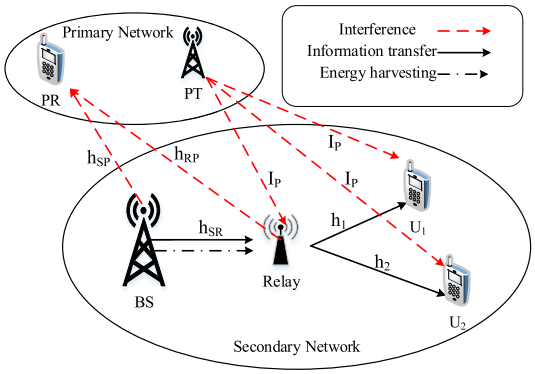

FIGURE 1. System model of EH-assisted CR-NOMA networks.

Notation: The cumulative distribution function (CDF) of a real-valued random variable X is denoted by $F_X(\cdot)$, $f_X(\cdot)$ stands for probability density functions (PDF), while $Pr(\cdot)$ symbolizes outage probability. $Ei(\cdot)$ is the exponential integral function.

II. SYSTEM MODEL

In Fig.1, a downlink cooperative underlay EH-assisted CR-NOMA is considered in this study. In this model, we only concern on performance of secondary network (SN) where consists of a secondary base station (node S), a relay (R) and two distant NOMA users (U_1, U_2) .[1] Such SN is able to operate together with primary network (PN) containing primary transmitter (PT) and primary destination (PR). Due to long transmission distance and poor channel condition in the secondary network, no direct exists in transmission between secondary transmitter (S) and secondary destinations (U_1, U_2). Two assumptions of wireless channels are studied, i.e. Rayleigh fading and Nakagami-*m* fading. We assume zero-mean additive white Gaussian noise samples of variance N_0 at all terminals. On the other hand, the energy-limited relay nodes adopt linear EH circuits to harvest energy from the BS and receive the information in the same time and then utilizes the harvested energy to forward signal to far NOMA users by implementing decode-and-forward (DF) based relay. Moreover the interference from the PT to the users and relay of the SN is denoted by I_P. It is assumed that $I_P \sim CN(0, N_0\varepsilon)$ as [34]. With regard to interference exists among two networks (SN, PN) these nodes are required the

[1] We limit the number of users to guarantee performance of each user and to guarantee QoS since degraded performance occurs due to interference among three or four users reported in [9].

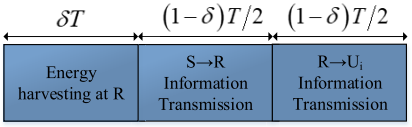

FIGURE 2. TS Mode: Transmission phase allocation.

TABLE 1. The channel of the system model.

Symbol	Description
x_i	The unit messages of user U_i
α_i	The power allocation coefficients for user U_i
P_S	The transmit power at S
η	The energy conversion efficiency of the EH circuitry satisfying $(0 < \eta < 1)$
ϑ	The power splitting factor in EH protocol
ρ_I	Set to I_{th}/N_0, where I_{th} is interference temperature constraint (ITC) at node PR [35] and N_0 is the variance of AWGN
h_{SR}	The Rayleigh fading channel of link BS - relay with $h_{SR} \sim CN(0, \lambda_{SR})$
h_{SP}	The Rayleigh fading channel of link BS-PR with $h_{SP} \sim CN(0, \lambda_{SP})$
h_{RP}	The Rayleigh fading channel of link Relay-PR with $h_{RP} \sim CN(0, \lambda_{RP})$
h_i	The Rayleigh fading channel of link relay-U_i with $h_i \sim CN(0, \lambda_i)$

secondary transmit node k is given $P_k \leq \frac{I_{th}}{|h_{kP}|^2}$, $k \in \{S, R\}$. The channel gains are considered as Table 1.

To implement NOMA transmission, the source S sends the signal $\sum_{i=1}^{2} \sqrt{P_S \alpha_i} x_i + n_R$ to the relay R according to NOMA. In this fixed power allocation scheme, $i \in \{1, 2\}$ α_i is the power allocation coefficients satisfying $\alpha_1 + \alpha_2 = 1$ and we call n_R as the additive white Gaussian noise (AWGN) between BS and R.

A. TIME SWITCHING RELAYING PROTOCOL (TS)

Without loss of generality, three time slots are divided to serve the transmission in duration T for TS mode and T is assumed to be unity as shown in Fig. 2. In the second time slot with time $(1-\delta)T/2$, $0 < \delta < 1$ after EH period of δT, a source BS sends data to relay R, and the last time slot is used to signal transmission to distant users. In this mode, the relay employs TS to perform EH. As a result, the energy accumulated at the relay during allocated time is given as [23]

$$E_S = \eta P_S |h_{SR}|^2 \delta T. \tag{1}$$

With period of allocated phase, the maximum available transmit power of relay which benefits from the harvested energy and the transmit power at R is given as

$$P_R^{TS} = \frac{E_S}{(1-\delta)\,T/2} = \frac{2\eta P_S |h_{SR}|^2 \delta}{(1-\delta)}, \tag{2}$$

Here, R is required to transmit signal with power $\bar{P}_R^{TS}$ which is constrained by both P_R^{TS} and I_{th} at PR. Therefore, the transmit power in R can be constrained by

$$\bar{P}_R^{TS} \leq \min\left\{P_R^{TS}, P_R\right\}. \tag{3}$$

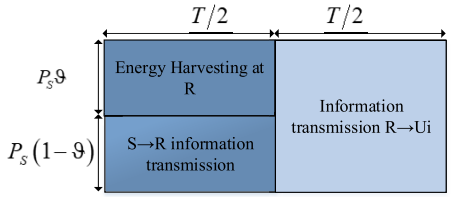

FIGURE 3. PS Mode: Transmission phase allocation.

In such CR-NOMA, the received signals at R can be expressed as

$$y_{SR}^{TS} = h_{SR}\sqrt{P_S}\left(\sqrt{\alpha_1}x_1 + \sqrt{\alpha_2}x_2\right) + I_P + n_R. \tag{4}$$

In the first phase, the signal to interference-plus-noise ratio (SINR) after treating x_1 as interference is given by

$$\gamma_{R,2}^{TS} = \frac{|h_{SR}|^2 \alpha_2 P_S}{|h_{SR}|^2 \alpha_1 P_S + N_0(\varepsilon + 1)}. \tag{5}$$

It is worth noting that imperfect SIC occurs, the SINR of detect x_2 is given as

$$\gamma_{R,1}^{TS} = \frac{P_S \alpha_1 |h_{SR}|^2}{P_S \alpha_2 |g_{SR}|^2 + N_0(\varepsilon + 1)}, \tag{6}$$

where $g_{SR} \sim CN(0, \zeta\lambda_{SR})$ with ζ $(0 \leqslant \zeta < 1)$ denotes as the level of residual interference caused by imperfect SIC. [2]

B. POWER SPLITTING RELAY PROTOCOL (PS)

Is this section, we consider the PS protocol and hence, the energy accumulated at the relay during fractional time $T/2$ is formulated as

$$\hat{E}_S = \eta P_S |g_{SR}|^2 \vartheta \frac{T}{2}, \tag{7}$$

Therefore, the maximum available transmit power of relay achieved from the harvested energy is given as

$$P_R^{PS} = \frac{\hat{E}_S}{T/2} = \eta P_S |h_{SR}|^2 \vartheta. \tag{8}$$

Similarly, the transmit power at R in this PS mode is determined by

$$\bar{P}_R^{PS} \leq \min\left\{P_R^{PS}, P_R\right\}. \tag{9}$$

By exploiting PS, it can be shown the received signal at R as

$$y_{SR}^{PS} = h_{SR}\sqrt{(1-\vartheta)P_S}\left(\sqrt{\alpha_1}x_1 + \sqrt{\alpha_2}x_2\right) + I_P + n_R. \tag{10}$$

In the first phase, the SINR to detect x_2 after treating x_1 as interference can be given as

$$\gamma_{R,2}^{PS} = \frac{|h_{SR}|^2 (1-\vartheta)\alpha_2 P_S}{|h_{SR}|^2 (1-\vartheta)\alpha_1 P_S + N_0(\varepsilon + 1)}. \tag{11}$$

[2]Here, the imperfect SIC model is adopted as in [24], where the imperfect SIC error follows Gaussian distribution.

Similarly, in the situation of imperfect SIC, the SINR to detect x_2 is given as

$$\gamma_{R,1}^{PS} = \frac{|h_{SR}|^2 (1-\vartheta)\alpha_1 P_S}{(1-\vartheta)\alpha_2 P_S |g_{SR}|^2 + N_0(\varepsilon+1)}. \quad (12)$$

C. SIGNAL PROCESSING IN THE SECOND PHASE

In the second phase using DF relaying mode, the received signal at $U_i, i = 1, 2$ in terms of TS and PS protocols and they can be formulated by

$$y_i^u = h_i \sqrt{\bar{P}_R^u}\left(\sqrt{\alpha_1}x_1 + \sqrt{\alpha_2}x_2\right) + I_P + n_i, \quad (13)$$

where $u \in \{TS, PS\}$, then user U_1 implements SIC by detecting x_2 while considering remaining signal x_1 as a noise. In this case, the SINR is given by

$$\gamma_{1,2}^u = \frac{\alpha_2 \bar{P}_R^u |h_1|^2}{\alpha_1 \bar{P}_R^u |h_1|^2 + N_0(\varepsilon+1)}. \quad (14)$$

With imperfect SIC, the SINR after treating x_2 as noise

$$\gamma_1^u = \frac{\alpha_1 \bar{P}_R^u |h_1|^2}{\alpha_2 \bar{P}_R^u |g_1|^2 + N_0(\varepsilon+1)}, \quad (15)$$

where $g_1 \sim CN(0, \zeta\lambda_1)$. Similarly, the SINR at U_2 is calculated by

$$\gamma_2^u = \frac{\alpha_2 \bar{P}_R^u |h_2|^2}{\alpha_1 \bar{P}_R^u |h_2|^2 + N_0(\varepsilon+1)}. \quad (16)$$

Remark 1: The system performance will depends on how each signal is detected at destinations. As observation in (14), (15), the first user employs the SIC to decode the desired message while the second user decodes its own signal by treating the interfering signal as a noise term in (16). In these expressions, power allocation factors α_1 and α_2 are main reason for performance gap among two users. We further verify such evaluation in simulation result section.

III. SCENARIO I: RAYLEIGH FADING

In this section, we examine the system performance in term of the outage probability in order to reveal the benefits of our proposed scheme.

Firstly, the PDF, CDF of wireless channel h_j with mean λ_j are defined respectively by

$$f_{h_j}(x) = \frac{1}{\lambda_j} e^{-\frac{x}{\lambda_j}}, \quad (17)$$

and

$$F_{h_j}(x) = 1 - e^{-\frac{x}{\lambda_j}}. \quad (18)$$

Then, we derive outage probability as main metric to evaluate system performance as following sections.

A. OUTAGE PERFORMANCE IN CASE OF TS

To successful detect signal x_1 at destination, it requires x_1 which can be detected at both relay, before SIC and after SIC operated at destinations. In particular, the outage probability of x_1 with imperfect SIC can be formulated as

$$OP_1^{TS} = 1 - \Pr\left\{\gamma_{R,2}^{TS} > \gamma_{th2}^{TS}, \gamma_{R,1}^{TS} > \gamma_{th1}^{TS}, \gamma_{1,2}^{TS} > \gamma_{th2}^{TS}, \gamma_1^{TS} > \gamma_{th1}^{TS}\right\}, \quad (19)$$

where $\gamma_{thi}^{TS} = 2^{2R_{thi}/(1-\delta)} - 1$ is the threshold SNR corresponding to target rates R_{thi} for two users; $R_{thi}, i = 1, 2$ as the target rate of user U_i.

Fortunately, to solve (19), the lower bound outage probability computation is performed, i.e., $OP_1^{TS} \approx OP_{1,lb}^{TS}$. Therefore, we continue to compute other lower bound of outage probability for many cases onward. Thus, $OP_{1,lb}^{TS}$ is rewritten as

$$OP_1^{TS} \approx OP_{1,lb}^{TS} = 1 - \Pr\left\{\gamma_{R,2}^{TS} > \gamma_{th2}^{TS}, \gamma_{R,1}^{TS} > \gamma_{th1}^{TS}\right\} \times \Pr\left\{\gamma_{1,2}^{TS} > \gamma_{th2}^{TS}, \gamma_1^{TS} > \gamma_{th1}^{TS}\right\}. \quad (20)$$

Next, the first and second term of (20) are denoted by $\Xi_1 = \Pr\left\{\gamma_{R,2}^{TS} > \gamma_{th2}^{TS}, \gamma_{R,1}^{TS} > \gamma_{th1}^{TS}\right\}$ and $\Xi_2 = \Pr\left\{\gamma_{1,2}^{TS} > \gamma_{th2}^{TS}, \gamma_1^{TS} > \gamma_{th1}^{TS}\right\}$. They can be derived as following the propositions.

Proposition 1: The first term Ξ_1 can be expressed as below

$$\Xi_1 = \mathcal{J}_1^{TS} - \frac{\mathcal{J}_2^{TS}\lambda_{SR}}{\mathcal{J}_3^{TS}\lambda_{SP} + \lambda_{SR}}, \quad (21)$$

where $\theta_1^{TS} = \frac{\gamma_{th1}^{TS}(\varepsilon+1)}{\rho_I \alpha_1}$, $\theta_2^{TS} = \frac{\gamma_{th2}^{TS}(\varepsilon+1)}{(\alpha_2 - \gamma_{th2}^{TS}\alpha_1)\rho_I}$, $\bar{\alpha} = \frac{\alpha_2}{\alpha_1}$, $\theta^{TS} = \max\left(\theta_1^{TS}, \theta_2^{TS}\right)$, $\zeta^{TS} = \zeta\gamma_{th1}^{TS}\bar{\alpha}$, $\mathcal{J}_1^{TS} = \frac{\lambda_{SR}}{\theta_1^{TS}\lambda_{SP} + \lambda_{SR}}$, $\mathcal{J}_2^{TS} = \frac{\zeta^{TS}}{\zeta^{TS}+1}$ and $\mathcal{J}_3^{TS} = \frac{(\zeta^{TS}+1)\theta^{TS} - \theta_1^{TS}}{\zeta^{TS}}$.

Proof: See Appendix A.

In addition, Ξ_2 is presented in Proposition 2 as below.

Proposition 2:

The second term Ξ_2 can be computed in closed-form as below

$$\Xi_2 = A_1 + A_2. \quad (22)$$

in which, A_1 and A_2 are expressed respectively by

$$A_1 = \mathcal{Q}_1^{TS}\Theta\left(\theta^{TS}\wp_1^{TS} + \mathcal{C}^{TS}\right) - \frac{\mathcal{J}_2^{TS}\lambda_1\Theta\left(\mathcal{J}_3^{TS}\wp_1^{TS} + \mathcal{C}^{TS}\right)}{\mathcal{J}_3^{TS}\lambda_{RP} + \lambda_1}, \quad (23)$$

where $\wp_i^{TS} = \frac{\lambda_{SP}}{\chi\lambda_1\lambda_{SR}}$, $\mathcal{C}^{TS} = \frac{\lambda_{SP}}{\chi\lambda_{RP}\lambda_{SR}}$ and $\Theta(x) = e^x\left(xE_1(-x) + e^{-x}\right)$,

$$A_2 = \Theta\left(\theta^{TS}\wp_1^{TS}\right) - \Theta\left(\theta^{TS}\wp_1^{TS} + \mathcal{C}^{TS}\right) - \mathcal{J}_2^{TS}\Theta\left(\mathcal{J}_3^{TS}\wp_1^{TS}\right) + \mathcal{J}_2^{TS}\Theta\left(\mathcal{J}_3^{TS}\wp_1^{TS} + \mathcal{C}^{TS}\right). \quad (24)$$

Proof: See Appendix B.

With the help of (21) and (22), we can obtain the closed-form expression for outage probability of x_1 as

$$OP_{1,lb}^{TS,I} = 1 - \Xi_1 \times \Xi_2. \tag{25}$$

By definition, we next examine the outage probability of x_2 and it can be expressed as

$$OP_2^{TS} \approx OP_{2,lb}^{TS} = 1 - \Pr\left(\gamma_2^{TS} > \gamma_{th2}^{TS}\right) \times \Pr\left(\gamma_{R,2}^{TS} > \gamma_{th2}^{TS}, \gamma_{R,1}^{TS} > \gamma_{th1}^{TS}\right) \tag{26}$$

We denote $\Xi_3 = \Pr\left(\gamma_2^{TS} > \gamma_{th2}^{TS}\right)$. Similarly, it can be solved Ξ_3 in Proposition 3.

Proposition 3: The closed-form expression for outage probability of Ξ_3 is expressed as

$$\Xi_3 = \mathcal{Q}_2^{TS}\Theta\left(\theta_2^{TS}\wp_2^{TS} + \mathcal{C}^{TS}\right) + \Theta\left(\theta_2^{TS}\wp_2^{TS}\right) - \Theta\left(\theta_2^{TS}\wp_2^{TS} + \mathcal{C}^{TS}\right). \tag{27}$$

Proof: With the help of (16), we can rewrite Ξ_3 as

$$\Xi_3 = \Pr\left(|h_2|^2 > \theta_2^{TS}|h_{RP}|^2, |h_{RP}|^2 > \frac{1}{\chi Z}\right) + \Pr\left(|h_2|^2 > \frac{\theta_2^{TS}}{Z\chi}, |h_{RP}|^2 < \frac{1}{\chi Z}\right). \tag{28}$$

Then, we can simplify Ξ_3 as

$$\Xi_3 = \int_0^\infty f_Z(z) \int_{\frac{1}{\chi z}}^\infty f_{|h_{RP}|}(x)\bar{F}_{|h_2|^2}\left(\theta_2^{TS}x\right)dxdz + \int_0^\infty f_Z(z)\bar{F}_{|h_2|^2}\left(\frac{\theta_2^{TS}}{z\chi}\right)dz - \int_0^\infty f_Z(z)\bar{F}_{|h_2|^2}\left(\frac{\theta_2^{TS}}{z\chi}\right)\bar{F}_{|h_{RP}|^2}\left(\frac{1}{\chi z}\right)dz. \tag{29}$$

Similarly, after some manipulations we obtain the closed-form expression for Ξ_3.

It completes the proof.

Finally, the outage probability of x_2 is given by

$$OP_{2,lb}^{TS,I} = 1 - \Xi_1 \times \Xi_3. \tag{30}$$

Remark 2: Although the exact expressions for the outage probability can been obtained, it is of great difficulty to achieve further insights. In this regard, a simpler bound for the outage probability should be calculated. Furthermore, the power allocation factors, channel gains and threshold SNR are main parameters which influence on outage performance of the considered system. These findings provide important guidelines to implement such system in practice.

B. CONSIDERATION ON OUTAGE PERFORMANCE IN CASE OF PS

Similarly, the outage probability of x_1 in PS mode is given by

$$OP_{1,lb}^{PS} = 1 - \underbrace{\Pr\left(\gamma_{R,2}^{PS} > \gamma_{th2}^{PS}, \gamma_{R,1}^{PS} > \gamma_{th1}^{PS}\right)}_{\Psi_1} \times \underbrace{\Pr\left(\gamma_{1,2}^{PS} > \gamma_{th2}^{PS}, \gamma_1^{PS} > \gamma_{th1}^{PS}\right)}_{\Psi_2}. \tag{31}$$

Substituting (11) and (12) into (31) we have

$$\Psi_1 = \Pr\left(\frac{|h_{SR}|^2}{|h_{SP}|^2} > \frac{\theta^{PS}}{(1-\vartheta)}, |h_{SR}|^2 > |g_{SR}|^2\gamma_{th1}^{PSR}\tilde{\alpha} + \frac{\theta^{PS}|h_{SP}|^2}{(1-\vartheta)}\right), \tag{32}$$

where $\theta_1^{PS} = \frac{\gamma_{th1}^{PS}(\varepsilon+1)}{\rho_I\alpha_1(1-\vartheta)}$, $\theta_2^{PS} = \frac{\gamma_{th2}^{PS}(\varepsilon+1)}{\rho_I(\alpha_2-\gamma_{th2}^{TS}\alpha_1)(1-\vartheta)}$ and $\theta^{PS} = \max\left(\theta_1^{PS}, \theta_2^{PS}\right)$. Similarly, Ψ_1 can be calculated as

$$\Psi_1 = \mathcal{J}_1^{PS} - \frac{\mathcal{J}_2^{PS}\lambda_{SR}}{\mathcal{J}_3^{PS}\lambda_{SP} + \lambda_{SR}}. \tag{33}$$

Then, with the help of (14) and (15) in case of PS scheme. It can be computed Ψ_2 as below

$$\begin{aligned}\Psi_2 &= \mathcal{Q}_1^{PS}\Theta\left(\theta^{PS}\wp_1^{PS} + \mathcal{C}^{PS}\right) - \frac{\mathcal{J}_2^{PS}\lambda_1\Theta\left(\mathcal{J}_3^{PS}\wp_1^{PS} + \mathcal{C}^{PS}\right)}{\mathcal{J}_3^{PS}\lambda_{RP} + \lambda_1} \\ &\quad + \Theta\left(\theta^{PS}\wp_1^{PS}\right) - \Theta\left(\theta^{PS}\wp_1^{PS} + \mathcal{C}^{PS}\right) \\ &\quad - \mathcal{J}_2^{PS}\Theta\left(\mathcal{J}_3^{PS}\wp_1^{PS}\right) + \mathcal{J}_2^{PS}\Theta\left(\mathcal{J}_3^{PS}\wp_1^{PS} + \mathcal{C}^{PS}\right),\end{aligned} \tag{34}$$

where $\mathcal{C}^{PS} = \frac{\lambda_{SP}}{\eta\vartheta\lambda_{RP}\lambda_{SR}}$ and $\wp_i^{PS} = \frac{\lambda_{SP}}{\eta\vartheta\lambda_i\lambda_{SR}}$. Next, the outage probability of x_2 in case of PS is expressed by

$$OP_{2,lb}^{PSR} = 1 - \underbrace{\Pr\left(\gamma_2^{PSR} > \gamma_{th2}^{PSR}\right)}_{\Psi_3} \times \Pr\left(\gamma_{R,2}^{PSR} > \gamma_{th2}^{PSR}, \gamma_{R,1}^{PSR} > \gamma_{th1}^{PSR}\right). \tag{35}$$

Similarly, Ψ_3 can be obtained as

$$\Psi_3 = \mathcal{Q}_2^{PS}\Theta\left(\theta_2^{PS}\wp_2^{PS} + \mathcal{C}^{PS}\right) + \Theta\left(\theta_2^{PS}\wp_2^{PS}\right) - \Theta\left(\theta_2^{PS}\wp_2^{PS} + \mathcal{C}^{TS}\right) \tag{36}$$

Finally, the outage probability of x_2 in PS can be expressed as

$$OP_{2,lb}^{PSR,I} = 1 - \Psi_2 \times \Psi_3 \tag{37}$$

C. ASYMPTOTIC OUTAGE BEHAVIOR ANALYSIS

The diversity order of x_i is given as [26]

$$d = -\lim_{\rho_I \to \infty} \frac{\log\left(OP_i^u\left(\rho_I\right)\right)}{\log\left(\rho_I\right)}, \tag{38}$$

where OP_i^u is denoted as the outage probability of x_i with u stands for either TS or PS. The asymptotic analysis when $\rho_I \to \infty$ depends on the achievable outage probabilities.

It is noted that $e^{-x} \approx 1 - x$ and $Ei(-x) = \ln(x) + C$ in [41, 3.351.4], where C is the Euler constant. Therefore, we can write $\Theta^\infty(x) = (1+x)(x(\ln(x)+C)+(1-x))$. Next, the asymptotic outage probability of x_1 and x_2 in TS and PS can be expressed in (39) and (40) shown in the top of the next page. Moreover, substituting (39) and (40) into (38), the diversity orders of U_i are equal to zeros.

$$\begin{aligned} OP_{1,lb}^{u,\infty} = 1 - \left(\mathcal{J}_1^u - \frac{\mathcal{J}_2^u\lambda_{SR}}{\mathcal{J}_3^u\lambda_{SP}+\lambda_{SR}}\right)\left(\mathcal{Q}_1^u\Theta^\infty\left(\theta^u\wp_1^u+\mathcal{C}^u\right)\right. \\ -\frac{\mathcal{J}_2^u\lambda_1\Theta^\infty\left(\mathcal{J}_3^u\wp_1^u+\mathcal{C}^u\right)}{\mathcal{J}_3^u\lambda_{RP}+\lambda_1} \\ +\Theta^\infty\left(\theta^u\wp_1^u\right)-\Theta^\infty\left(\theta^u\wp_1^u+\mathcal{C}^u\right) \\ \left.-\mathcal{J}_2^u\Theta^\infty\left(\mathcal{J}_3^u\wp_1^u\right)+\mathcal{J}_2^u\Theta^\infty\left(\mathcal{J}_3^u\wp_1^u+\mathcal{C}^{TSu}\right)\right), \end{aligned} \tag{39}$$

$$\begin{aligned} OP_{2,lb}^{u,\infty} = 1 - \left(\mathcal{J}_1^u - \frac{\mathcal{J}_2^u\lambda_{SR}}{\mathcal{J}_3^u\lambda_{SP}+\lambda_{SR}}\right)\left(\mathcal{Q}_2^u\Theta^\infty\left(\theta_2^u\wp_2^u+\mathcal{C}^u\right)\right. \\ \left.+\Theta^\infty\left(\theta_2^m\wp_2^u\right)-\Theta^\infty\left(\theta_2^u\wp_2^u+\mathcal{C}^u\right)\right). \end{aligned} \tag{40}$$

IV. SCENARIO II: NAKAGAMI-*m* FADING

In this section, we examine the system performance in terms of outage probability in order to reveal the benefits of our proposed scheme.

Firstly, the PDF and CDF of wireless channel h_j with ($j \in SR, SP, RP, 1, 2$) are defined respectively by

$$f_{|h_j|^2}(x) = \frac{x^{m_j-1}e^{-\frac{x}{\Omega_j}}}{\Gamma\left(m_j\right)\Omega_j^{m_j}}, \tag{41}$$

and

$$\begin{aligned} F_{|h_j|^2}(x) &= 1 - \frac{\Gamma\left(m_j, x/\Omega_j\right)}{\Gamma\left(m_j\right)} \\ &= 1 - e^{-\frac{x}{\Omega_j}}\sum_{i=0}^{m_j-1}\frac{1}{i!}\left(\frac{x}{\Omega_j}\right)^i, \end{aligned} \tag{42}$$

where $\Omega_j = \frac{\lambda_j}{m_j}$, m_j represents the fading severity factor. In this paper, we also assume m_j as an integer number and $m_j \geqslant 1$. The equality in (42) is achieved by applying an equivalent relationship in [42, Eq.8.352.6].

A. OUTAGE PERFORMANCE IN CASE OF TS

To successful detect signal x_1 at destination, it is necessary to x_1 which can be detected at relay in two situation, i.e., before SIC and after SIC operated at the destinations. In particular, the outage probability of x_1 with imperfect SIC can be formulated as

$$\begin{aligned} OP_{1,lb}^{TS} = 1 - \Pr\left\{\gamma_{R,2}^{TS} > \gamma_{th2}^{TS}, \gamma_{R,1}^{TS} > \gamma_{th1}^{TS}\right\} \\ \times \Pr\left\{\gamma_{1,2}^{TS} > \gamma_{th2}^{TS}, \gamma_1^{TS} > \gamma_{th1}^{TS}\right\}, \end{aligned} \tag{43}$$

where $\gamma_{thi}^{TS} \triangleq 2^{\frac{2R_{thi}}{1-\delta}} - 1$ is the decoding threshold of x_i corresponding to target rates R_{thi} for the user U_i, $i = 1, 2$.

Proposition 4: In this case, we denote the first and the second probability term in (43) as $\bar{\Xi}_1$ and $\bar{\Xi}_2$, respectively. Then, $\bar{\Xi}_1$ can be obtained by

$$\begin{aligned} \bar{\Xi}_1 = \sum_{i=0}^{m_{SR}-1}\binom{m_{SP}+i-1}{m_{SP}-1}\frac{\bar{\Omega}^{m_{SP}}\theta^i}{\left(\bar{\Omega}+\theta\right)^{m_{SP}+i}} \\ -\sum_{i=0}^{m_{SR}-1}\sum_{p=0}^{i}\sum_{k=0}^{m_{SR}+i-p-1}\binom{m_{SR}+i-p-1}{m_{SR}-1} \\ \times\frac{\Gamma\left(m_{SP}+p+k\right)\left(\zeta_1^{TS}\right)^{m_{SR}+m_{SP}}}{p!k!\Gamma\left(m_{SP}\right)\left(1+\zeta_1^{TS}\right)^{m_{SR}+i-p-k}} \\ \times\frac{(-1)^p\left(\theta_1^{TS}\right)^p\theta^k\bar{\Omega}^{m_{SP}}}{\left(\bar{\Omega}\zeta_1^{TS}-\theta_1^{TS}+\theta+\zeta_1^{TS}\theta\right)^{m_{SP}+p+k}}. \end{aligned} \tag{44}$$

Proof: See Appendix C.

Lemma 1: Denote $Z \triangleq \frac{|h_{SR}|^2}{|h_{SP}|^2}$ as the ratio of two Gamma random variables, the CDF of Z with $\gamma > 0$ can be expressed as

$$\begin{aligned} F_Z(\gamma) = 1 - \sum_{m=0}^{m_{SR}-1}\binom{m_{SR}+m-1}{m_{SR}-1} \\ \times\frac{(\gamma\Omega_{SP})^m(\Omega_{SR})^{m_{SP}}}{(\gamma\Omega_{SP}+\Omega_{SR})^{m_{SP}+m}}. \end{aligned} \tag{45}$$

By taking the first derivative of (45), the corresponding PDF can be obtained with $\gamma > 0$ as

$$f_Z(\gamma) = \frac{(m_{SR}+m_{SP}-1)!}{\Upsilon}\times\frac{\Omega_{SR}^{m_{SP}}\Omega_{SP}^{m_{SR}}}{(\Omega_{SP}\gamma+\Omega_{SR})^{m_{SR}+m_{SP}}}\gamma^{m_{SR}-1}, \tag{46}$$

where $\Upsilon = (m_{SR}-1)!\,(m_{SP}-1)!$. Note that the CDF and PDF of the random variable Z^{-1} can be obtained through (45) and (46) by simple changing the subscript SR to SP and vice versa.

Lemma 2: For a set of parameters $n \geq 1$, $\beta > 0$, $\mu > 0$, the

$$\mathcal{P} = \int_0^\infty \frac{x^{v-1}}{(x+\beta)^n}e^{-\mu x}dx = \frac{\beta^{v-n}}{\Gamma(n)}G_{1,2}^{2,1}\left[\begin{matrix}1-v\\0,n-v\end{matrix}\middle|\,\beta\mu\right]. \tag{47}$$

Proposition 5: Moreover, the closed-form expression of $\bar{\Xi}_2$ can be written as

$$\bar{\Xi}_2 = B_1 + B_2. \tag{48}$$

It is noted that $B_1 = B_{1,1} - B_{1,2}$, where $B_{1,1}$ and $B_{1,2}$ are expressed respectively by

$$B_{1,1} = \sum_{i=0}^{m_1-1}\sum_{p=0}^{m_{RP}+i-1}\binom{m_{RP}+i-1}{m_{RP}-1} \times \frac{(I_1)^{m_{RP}-p}}{p!\Upsilon\left(\bar{\Omega}\Omega_{RP}\chi\right)^p(I_1+1)^{m_{RP}+i-p}} \times G_{2,1}^{1,2}\left[1-m_{SP}-p,\ 0,\ m_{SR}-p \,\middle|\, \frac{I_1+1}{I_1\Omega_{RP}\bar{\Omega}\chi}\right], \quad (49)$$

$$B_{1,2} = \sum_{i=0}^{m_j-1}\sum_{p=0}^{i}\sum_{k=0}^{m_1+i-p-1}\sum_{n=0}^{m_{RP}+p+k-1}\binom{m_1+i-p-1}{m_1-1} \times \frac{\Gamma\left(m_{RP}+p+k\right)\left(\theta^{TS}\right)^{m_{RP}+k}(I_1)^{m_{RP}}}{\Upsilon p!k!n!\Gamma\left(m_{RP}\right)\left(\bar{\Omega}\Omega_1\chi\right)^n\left(\zeta^{TS}+1\right)^{m_1+i-p-k}} \times \frac{(-1)^p\left(\theta_1^{TS}\right)^p\left(\zeta^{TS}\right)^{m_{RP}+m_1-n}}{\left(\theta I_1\zeta^{TS}-\theta_1^{TS}+\theta^{TS}\zeta^{TS}+\theta^{TS}\right)^{m_{RP}+p+k-n}} \times G_{1,2}^{2,1}\left[1-m_{SP}-n,\ 0,\ m_{SR}-n \,\middle|\, \frac{I_1\theta\zeta_1^{TS}-\theta_1^{TS}+\theta^{TS}\zeta^{TS}+\theta^{TS}}{\zeta^{TS}\bar{\Omega}\Omega_1\chi}\right]. \quad (50)$$

In this case, $B_2 = B_{2,1} - B_{2,2} - B_{2,3} + B_{2,4}$ and corresponding computations are follows

$$B_{2,1} = \sum_{i=0}^{m_1-1}\frac{1}{i!\Upsilon\left(I_1\Omega_{RP}\chi\bar{\Omega}\right)^i} \times G_{2,1}^{1,2}\left[1-m_{SP}-i,\ 0,\ m_{SR}-i \,\middle|\, \frac{1}{I_1\Omega_{RP}\bar{\Omega}\chi}\right], \quad (51)$$

$$B_{2,2} = \sum_{i=0}^{m_1-1}\sum_{p=0}^{m_{RP}-1}\frac{\left(\bar{\Omega}\Omega_{RP}\chi\right)^{-i-p}}{p!i!\Upsilon(I_1)^i} \times G_{2,1}^{1,2}\left[1-m_{SP}-i-p,\ 0,\ m_{SR}-i-p \,\middle|\, \frac{I_1+1}{I_1\bar{\Omega}\Omega_{RP}\chi}\right], \quad (52)$$

$$B_{2,3} = \sum_{i=0}^{m_1-1}\sum_{p=0}^{i}\sum_{k=0}^{m_1+i-p-1}\binom{m_1+i-p-1}{m_1-1} \times \frac{(-1)^p\left(\theta_1^{TS}\right)^p\left(\theta^{TS}\right)^k\left(\zeta^{TS}\right)^{m_1-p-k}}{p!k!\Upsilon\left(\chi\bar{\Omega}\Omega_1\right)^{p+k}\left(\zeta^{TS}+1\right)^{m_1+i-p-k}} \times G_{2,1}^{1,2}\left[1-m_{SP}-p-k,\ 0,\ m_{SR}-p-k \,\middle|\, \frac{\zeta^{TS}\theta^{TS}+\theta^{TS}-\theta_1^{TS}}{\chi\bar{\Omega}\Omega_1\zeta^{TS}}\right], \quad (53)$$

$$B_{2,4} = \sum_{i=0}^{m_1-1}\sum_{p=0}^{m_{RP}-1}\sum_{n=0}^{i}\sum_{l=0}^{m_1+i-n-1}\binom{m_1+i-n-1}{m_1-1} \times \frac{(-1)^n\left(\zeta^{TS}\right)^{m_1-n-l}\left(\theta_1^{TS}\right)^n\left(\theta^{TS}\right)^l}{\Upsilon p!n!l!(\Omega_{RP})^p\Omega_1^{n+l}\left(\bar{\Omega}\chi\right)^{p+n+l}\left(\zeta^{TS}+1\right)^{m_1+i-n-l}} \times G_{2,1}^{1,2}\left[1-m_{SP}-p-n-l,\ 0,\ m_{SR}-p-n-l \,\middle|\, \frac{I_1\theta^{TS}\zeta^{TS}+\theta^{TS}\zeta^{TS}+\theta^{TS}-\theta_1^{TS}}{\Omega_1\bar{\Omega}\chi\zeta^{TS}}\right]. \quad (54)$$

Proof: See Appendix D.

Finally, the closed-form outage probability of x_1 can be expressed as

$$OP_{1,lb}^{TS} = 1 - \bar{\Xi}_1 + \bar{\Xi}_2. \quad (55)$$

By definition, we next examine the outage probability of x_2 and it can be expressed as

$$OP_{2,lb}^{TS} = 1 - \Pr\left(\gamma_2^{TS} > \gamma_{th2}^{TS}\right) \times \Pr\left(\gamma_{R,2}^{TS} > \gamma_{th2}^{TS}, \gamma_{R,1}^{TS} > \gamma_{th1}^{TS}\right). \quad (56)$$

Proposition 6: Firstly, we define $\bar{\Xi}_3 = \Pr\left(\gamma_2^{TS} > \gamma_{th2}^{TS}\right)$. Then, it can be solved $\bar{\Xi}_3$ in the closed-form expression as

$$\bar{\Xi}_3 = C_1 - C_2 + C_3, \quad (57)$$

where C_1, C_1 and C_3 are written as below.

Proof:

Based on (28), it is written as

$$\Xi_3 = \int_0^\infty f_{Z^{-1}}(z)\bar{F}_{|h_2|^2}\left(\frac{\theta_2^{TS}z}{\chi}\right)dz - \int_0^\infty f_{Z^{-1}}(z)\bar{F}_{|h_2|^2}\left(\frac{\theta_2^{TS}z}{\chi}\right)\bar{F}_{|h_{RP}|^2}\left(\frac{z}{\chi}\right)dz + \int_0^\infty f_{Z^{-1}}(z)\int_{\frac{z}{\chi}}^\infty f_{|h_{RP}|^2}(x)\bar{F}_{|h_2|^2}\left(\theta_2^{TS}x\right)dxdz. \quad (58)$$

First, we continue to compute C_1, C_2 and C_3 terms in (57). Accordingly, C_1 can be calculated as

$$C_1 = \sum_{i=0}^{m_2-1}\frac{1}{i!\Upsilon\left(I_2\bar{\Omega}\Omega_{RP}\chi\right)^i} \times G_{2,1}^{1,2}\left[1-m_{SP}-i,\ 0,\ m_{SR}-i \,\middle|\, \frac{1}{\bar{\Omega}\chi\Omega_{RP}I_2}\right], \quad (59)$$

where $I_2 = \frac{\Omega_2}{\Omega_{RP}\theta_2^{TS}}$. Then, C_2 is given as

$$C_2 = \sum_{i=0}^{m_{RP}-1}\sum_{n=0}^{m_2-1}\frac{(I_2)^{-n}}{i!n!\Upsilon\left(\Omega_{RP}\bar{\Omega}\chi\right)^{i+n}} \times G_{2,1}^{1,2}\left[1-m_{SP}-i-n,\ 0,\ m_{SR}-i-n \,\middle|\, \frac{I_2+1}{I_2\Omega_{RP}\bar{\Omega}\chi}\right]. \quad (60)$$

In final step, C_3 can be achieved as

$$C_3 = \sum_{i=0}^{m_2-1}\sum_{p=0}^{m_{RP}+i-1}\binom{m_{RP}+i-1}{m_{RP}-1}$$

$$\times \frac{(I_2)^{m_{RP}-p}(1+I_2)^{-m_{RP}+p-i}}{p!\Upsilon\left(\chi\bar{\Omega}\Omega_{RP}\right)^p} \times G_{2,1}^{1,2}\left[\begin{matrix}1-m_{SP}-p\\0,m_{SR}-p\end{matrix}\middle|\frac{1+I_2}{I_2\Omega_{RP}\bar{\Omega}\chi}\right]. \quad (61)$$

It completes the proof.

Proposition 7: It can be computed outage performance of x_2 as

$$OP_{2,lb}^{TS} = 1 - \bar{\Xi}_1 \times \bar{\Xi}_3. \quad (62)$$

Proof: Using results from Proposition 3 and combining with (45), it leads to the final result.

It is the end of the proof.

B. CONSIDERATION ON OUTAGE PERFORMANCE IN CASE OF PS

Similarly, the outage probability of x_1 in PS mode with $\gamma_{thi}^{PS} \triangleq 2^{2R_{thi}} - 1$ is given by

$$OP_{1,lb}^{PS} = 1 - \underbrace{\Pr\left(\gamma_{R,2}^{PS} > \gamma_{th2}^{PS}, \gamma_{R,1}^{PS} > \gamma_{th1}^{PS}\right)}_{\bar{\Psi}_1} \times \underbrace{\Pr\left(\gamma_{1,2}^{PS} > \gamma_{th2}^{PS}, \gamma_1^{PS} > \gamma_{th1}^{PS}\right)}_{\bar{\Psi}_2}. \quad (63)$$

The first term in (63), Ψ_1 can be formulated as

$$\bar{\Psi}_1 = \Pr\left(\frac{|h_{SR}|^2}{|h_{SP}|^2} > \frac{\theta^{PS}}{(1-\vartheta)}, |g_{SR}|^2 < \frac{|h_{SR}|^2 - \frac{\theta_1^{PS}|h_{SP}|^2}{(1-\vartheta)}}{\gamma_{th1}^{PS}\tilde{\alpha}}\right). \quad (64)$$

In next step, Ψ_1 can be computed by

$$\bar{\Psi}_1 = \sum_{i=0}^{m_{SR}-1}\binom{m_{SP}+i-1}{m_{SP}-1}\frac{\left(\bar{\Omega}(1-\vartheta)\right)^{m_{SP}}(\theta^{PS})^i}{\left(\bar{\Omega}(1-\vartheta)+\theta^{PS}\right)^{m_{SP}+i}} - \sum_{i=0}^{m_{SR}-1}\sum_{p=0}^{i}\sum_{k=0}^{m_{SR}+i-p-1}\binom{m_{SR}+i-p-1}{m_{SR}-1} \times \frac{\Gamma(m_{SP}+p+k)\left(\bar{\Omega}(1-\vartheta)\right)^{m_{SP}}}{p!k!\Gamma(m_{SP})\left(1+\zeta^{TS}\right)^{m_{SR}+i-p-k}} \times \frac{(-1)^p\left(\theta_1^{PS}\right)^p\left(\theta^{PS}\right)^k\left(\zeta^{PS}\right)^{m_{SR}+m_{SP}}}{\left(\bar{\Omega}\zeta^{PS}(1-\vartheta)-\theta_1^{PS}+\theta^{PS}+\zeta^{PS}\bar{\theta}\right)^{m_{SP}+p+k}}. \quad (65)$$

Similarly, the second term of (63), $\bar{\Psi}_2$ can be obtained as $\Psi_2 = \Phi_1 + \Phi_2$. It is noted that, $I_3 = \frac{\Omega_1}{\Omega_{RP}\theta^{PS}}$, $I_4 = \frac{\Omega_2}{\Omega_{RP}\theta_2^{PS}}$, Φ_1 and Φ_2 are given as (66) and (67), shown in the top of the next top page.

$$\Phi_1 = \sum_{i=0}^{m_1-1}\sum_{p=0}^{m_{RP}+i-1}\binom{m_{RP}+i-1}{m_{RP}-1}\frac{(I_3)^{m_{RP}-p}\left(\bar{\Omega}\Omega_{RP}\eta\vartheta\right)^{-p}}{p!\Upsilon(I_3+1)^{m_{RP}+i-p}} \times G_{2,1}^{1,2}\left[\begin{matrix}1-m_{SP}-p\\0,m_{SR}-p\end{matrix}\middle|\frac{I_3+1}{I_3\Omega_{RP}\bar{\Omega}\eta\vartheta}\right] - \sum_{i=0}^{m_1-1}\sum_{p=0}^{i}\sum_{k=0}^{m_1+i-p-1}\sum_{n=0}^{m_{RP}+p+k-1}\binom{m_1+i-p-1}{m_1-1} \times \frac{(-1)^p(\theta^{PS})^{m_{RP}+k}(I_3)^{m_{RP}}\Gamma(m_{RP}+p+k)}{\Upsilon p!k!n!\Gamma(m_{RP})\left(\zeta^{PS}+1\right)^{m_1+i-p-k}\left(\bar{\Omega}\Omega_1\eta\vartheta\right)^n} \times \frac{\left(\theta_1^{PS}\right)^p\left(\zeta^{PS}\right)^{m_{RP}+m_1-n}}{\left(\theta^{PS}I_3\zeta^{PS}-\theta_1^{PS}+\theta^{PS}\zeta^{PS}+\theta^{PS}\right)^{m_{RP}+p+k-n}} \times G_{2,1}^{1,2}\left[\begin{matrix}1-m_{SP}-n\\0,m_{SR}-n\end{matrix}\middle|\frac{I_3\theta^{PS}\zeta^{PS}-\theta_1^{PS}+\theta^{PS}\zeta^{PS}+\theta^{PS}}{\zeta^{PS}\bar{\Omega}\Omega_1\eta\vartheta}\right]. \quad (66)$$

$$\Phi_2 = \sum_{i=0}^{m_1-1}\frac{\left(I_3\Omega_{RP}\bar{\Omega}\eta\vartheta\right)^{-i}}{i!\Upsilon}G_{2,1}^{1,2}\left[\begin{matrix}1-m_{SP}-i\\0,m_{SR}-i\end{matrix}\middle|\frac{1}{I_3\Omega_{RP}\bar{\Omega}\eta\vartheta}\right] - \sum_{i=0}^{m_1-1}\sum_{p=0}^{m_{RP}-1}\frac{\left(\bar{\Omega}\Omega_{RP}\eta\vartheta\right)^{-i-p}}{p!i!\Upsilon(I_3)^i} \times G_{2,1}^{1,2}\left[\begin{matrix}1-m_{SP}-i-p\\0,m_{SR}-i-p\end{matrix}\middle|\frac{I_3+1}{I_3\bar{\Omega}\Omega_{RP}\eta\vartheta}\right] - \sum_{i=0}^{m_1-1}\sum_{p=0}^{i}\sum_{k=0}^{m_1+i-p-1}\binom{m_1+i-p-1}{m_1-1} \times \frac{(-1)^p\left(\theta_1^{PS}\right)^p\left(\theta^{PS}\right)^k\left(\zeta^{PS}\right)^{m_1-p-k}}{p!k!\Upsilon\left(\bar{\Omega}\Omega_1\eta\vartheta\right)^{p+k}\left(\zeta^{PS}+1\right)^{m_1+i-p-k}} \times G_{2,1}^{1,2}\left[\begin{matrix}1-m_{SP}-p-k\\0,m_{SR}-p-k\end{matrix}\middle|\frac{\zeta^{PS}\theta^{PS}+\theta^{PS}-\theta_1^{PS}}{\bar{\Omega}\Omega_1\eta\vartheta\zeta^{PS}}\right] + \sum_{i=0}^{m_1-1}\sum_{p=0}^{m_{RP}-1}\sum_{n=0}^{i}\sum_{l=0}^{m_1+i-n-1}\binom{m_1+i-n-1}{m_1-1} \times \frac{(-1)^n\left(\zeta^{PS}\right)^{m_1-n-l}}{\Upsilon p!n!l!\Omega_{RP}^p\Omega_1^{n+l}} \times G_{2,1}^{1,2}\left[\begin{matrix}1-m_{SP}-p-n-l\\0,m_{SR}-p-n-l\end{matrix}\middle|\frac{I_3\bar{\theta}\zeta^{PS}+\bar{\theta}\zeta^{PS}+\bar{\theta}-\theta_1^{PS}}{\Omega_1\bar{\Omega}\eta\vartheta\zeta^{PS}}\right] \times \frac{\left(\theta_1^{PS}\right)^n\bar{\theta}^l}{\left(\zeta^{PS}+1\right)^{m_1+i-n-l}\left(\bar{\Omega}\eta\vartheta\right)^{p+n+l}}. \quad (67)$$

The outage probability of x_1 in PS mode can be achieved as follow

$$OP_{1,lb}^{PS} = 1 - \bar{\Psi}_1 \times \bar{\Psi}_2. \quad (68)$$

We further define outage behavior of x_2 in PS mode as

$$OP_{2,lb}^{PS} = 1 - \Pr\left(\gamma_2^{PS} > \gamma_{th2}^{PS}\right) \times \Pr\left(\gamma_{R,2}^{PS} > \gamma_{th2}^{PS}, \gamma_{R,1}^{PS} > \gamma_{th1}^{PS}\right). \quad (69)$$

Similarly, we denote $\bar{\Psi}_3 = \Pr\left(\gamma_2^{PS} > \gamma_{th2}^{PS}\right)$. Then, the closed-form expression of $\bar{\Psi}_3$ can be given as (70), shown

in the middle of the next page.

$$\bar{\Psi}_3 = \sum_{i=0}^{m_2-1} \frac{\left(I_4\bar{\Omega}\Omega_{RP}\eta\vartheta\right)^{-i}}{i!\Upsilon} G_{2,1}^{1,2}\left[\begin{matrix}1-m_{SP}-i\\0, m_{SR}-i\end{matrix}\middle|\frac{1}{\bar{\Omega}\Omega_{RP}\eta\vartheta I_4}\right] - \sum_{i=0}^{m_{RP}-1}\sum_{n=0}^{m_2-1} \frac{\left(\bar{\Omega}\Omega_{RP}\eta\vartheta\right)^{-i-n}}{i!n!\Upsilon I_4^n} \times G_{2,1}^{1,2}\left[\begin{matrix}1-m_{SP}-i-n\\0, m_{SR}-i-n\end{matrix}\middle|\frac{I_4+1}{I_4\bar{\Omega}\Omega_{RP}\eta\vartheta}\right] + \sum_{i=0}^{m_2-1}\sum_{p=0}^{m_{RP}+i-1} \binom{m_{RP}+i-1}{m_{RP}-1} \frac{I_4^{m_{RP}-p}\left(\bar{\Omega}\Omega_{RP}\eta\vartheta\right)^{-p}}{p!\Upsilon(1+I_4)^{m_{RP}+i-p}} \times G_{2,1}^{1,2}\left[\begin{matrix}1-m_{SP}-p\\0, m_{SR}-p\end{matrix}\middle|\frac{1+I_4}{I_4\bar{\Omega}\Omega_{RP}\eta\vartheta}\right]. \quad (70)$$

Now, the outage probability of x_2 can obtained as

$$OP_{2,lb}^{PS} = 1 - \bar{\Psi}_1 \times \bar{\Psi}_3. \quad (71)$$

V. THROUGHPUT PERFORMANCE

It can be further evaluated other metric, i.e. the overall throughput can be achieved based on obtained outage probabilities. In delay-limited mode, at fixed target rates R_{th1}, R_{th2} the throughput can be achieved. As a result, the overall throughput can be formulated as

$$T_{total}^{u} = \left(1 - OP_{1,lb}^{u}\right) R_{th1} + \left(1 - OP_{2,lb}^{u}\right) R_{th2}. \quad (72)$$

VI. NUMERICAL RESULTS

In this section, to verify mathematical analysis, it is necessary to simulate and illustrate for proposed EH assisted CR-NOMA scheme. In this circumstance, the Nakagami-m fading channel model is performed to model the wireless channels. Moreover, we also simulate the linear harvesting model as intuitively indications shown in each figure. We set power allocation factors $\alpha_2 = 0.8$, $\alpha_1 = 0.2$, the target rates $R_{th} = R_{th1} = R_{th2} = 0.5$ bit per channel use (BPCU) except for specific cases, $\varepsilon = 0.5$, the channel gains $\lambda_{SP} = \lambda_{RP} = 0.1$, $\lambda_{SR} = \lambda_2 = 1$, $\lambda_1 = 2$ and $m = m_{SR} = m_{SP} = m_{RP} = m_1 = m_2$. Moreover, case of $m = 1$ is equivalent with the Rayleigh fading channel model. In these following figures, Monte-Carlo simulations are performed to validate the analytical results.

The analytical and simulated outage probabilities for TS and PS schemes in the CR-NOMA system are shown in Fig. 4, Fig. 5. To provide an objective evaluation, the outage probabilities for a special case of high ρ_I are also provided. Such error floor lines confirmed the exactness of derived expressions. Outage performance in our paper is better in results reported in [40] at high ρ_I region. The performance gaps among two users for TS and PS scheme depend on power allocation factors (α_1, α_2) and ρ_I. It is further confirmed that CR-NOMA is better than CR-OMA in term of outage probability. Such outage behavior will be improved at higher transmit power ρ_I (it depends on I_{th}). This can be explained as follows: at higher SNR values, two destinations (users) receive a stronger signal to detect the desired signals, and

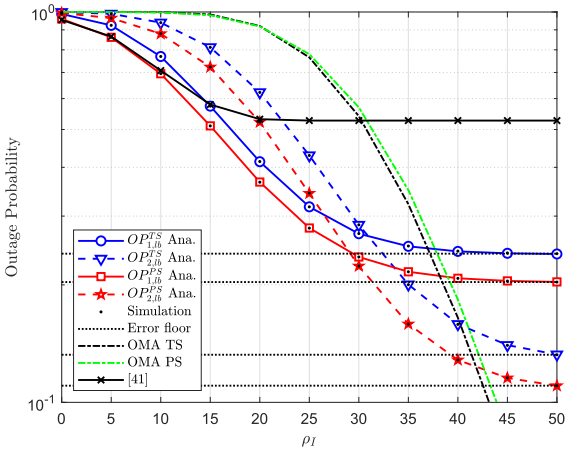

FIGURE 4. The outage probability versus transmit ρ_I with different values of R_{th}, where $\zeta = 0.01$, $\vartheta = 0.1$, $\delta = 0.1$, $\eta = 0.9$ and $m = 1$.

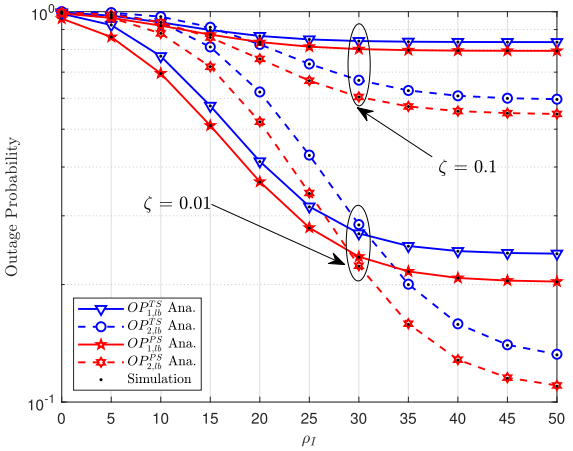

FIGURE 5. The outage probability versus transmit ρ_I with different values of ζ, where $\vartheta = 0.1$, $\delta = 0.1$, $\eta = 0.9$, $R_{th} = 0.5$ BPCU and $m = 1$.

hence they provide less possibility of outage event. The considered outage performance in CR-NOMA system using PS scheme outperforms than that of TS scheme at whole range of ρ_I. In general, it can be seen slight performance gap among two schemes (TS and PS). These illustrations show that error floor matches analytical curves at very high ρ_I, it confirms exactness of our derived expressions. Performance of the first user is better than that of the first user when ρ_I is less than 30 and this observation changes as ρ_I overcome 30. The main reason is that that the first user applies the SIC procedure to decode the desired message in (14), (15) (which intuitively provides us with higher SNR value) while the second user decodes its own signal by treating the interfering signal as a noise term in (16). Furthermore, it is evident that the analytical curves match well with the simulated results. Fig. 5 also shows similar trends of outage probability, but it indicates how imperfect SIC affects outage performance. For example, $\zeta = 0.1$ raises the worse performance compared with case of $\zeta = 0.01$. While impact of amount of harvested energy on outage event can be clear seen in Fig. 6. As $\eta = 0.7$,

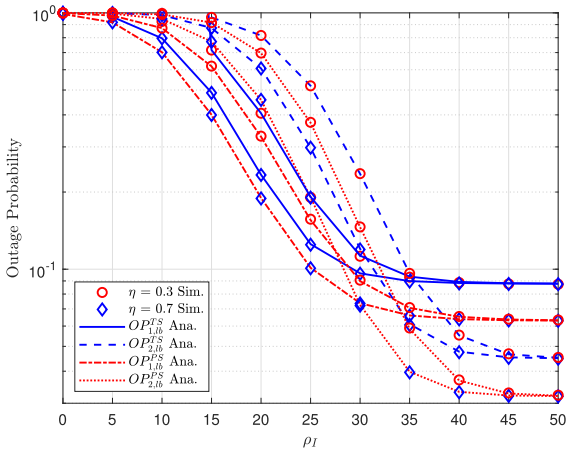

FIGURE 6. The outage probability versus transmit ρ_I with different values of η, where $\vartheta = 0.1$, $\delta = 0.1$, $\zeta = 0.01$, $R_{th} = 1$ BPCU and $m = 1$.

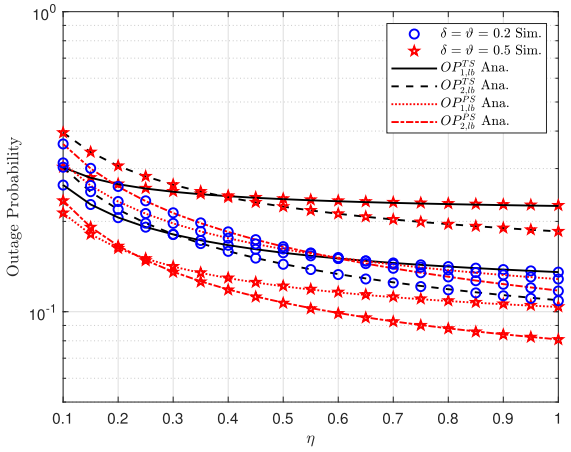

FIGURE 7. The outage probability versus η with different values of $\vartheta = \delta$, where $\rho_I = 20$ dB, $\zeta = 0.01$, $R_{th} = 0.5$ BPCU and $m = 1$.

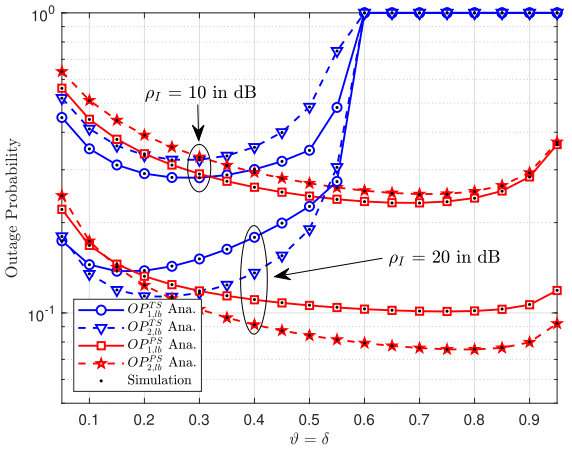

FIGURE 8. The outage probability versus $\vartheta = \delta$ with different values of ρ_I, where $\eta = 0.9$, $\zeta = 0.01$, $R_{th} = 0.5$ BPCU and $m = 1$.

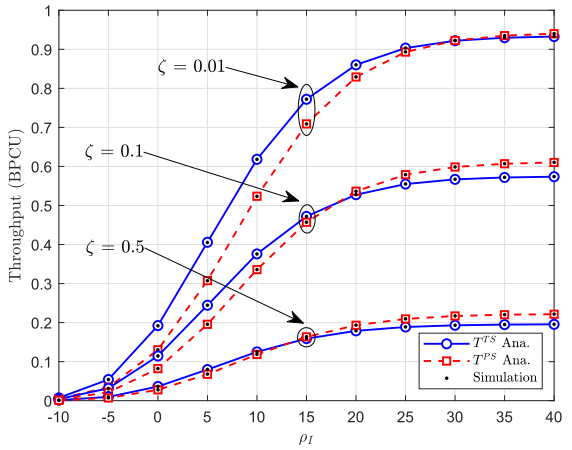

FIGURE 9. The Throughput versus transmit ρ_I with different values of ζ, where $\vartheta = 0.1$, $\delta = 0.1$, $\eta = 0.9$, $R_{th} = 0.5$ BPCU and $m = 1$.

better outage event for both users in two modes of EH can be achieved. Moreover, as the system SNR increases, the outage probability decreases and then reaches a fixed level, which leads the diversity order turns to zero. Such an observation is confirmed results derived in (38).

The slight performance change of two users versus EH efficiency factors η can be observed as in Fig. 8, it can be confirmed in wide range of $0 < \eta < 1$. Different $\vartheta = \delta$ corresponding to two main parts, i.e. EH and information processing, leads to varying outage behavior. It can be seen that equal allocation for functions of EH and information processing exhibits better outage performance. The main reason is that the proposed CR-NOMA can balances roles to achieve wireless power and signal processing. It can be predicted that existence optimal $\vartheta = \delta$ to happen lowest outage performance. Interestingly, the optimal performance can be obtained, as varying $\vartheta = \delta$ from 0 to 1, it can be obtained minimum points of outage events for two users in two cases $\rho_I = 10(dB)$, $\rho_I = 20(dB)$.

In term of overall throughput, level of imperfect SIC contributes to increasing throughput as increasing ρ_I.

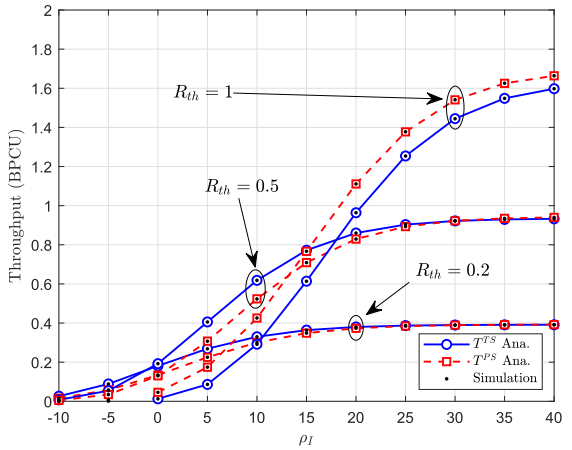

FIGURE 10. The Throughput versus transmit ρ_I with different values of R_{th}, where $\vartheta = 0.1$, $\delta = 0.1$, $\eta = 0.9$, $\zeta = 0.01$, $R_{th} = 0.5$ BPCU and $m = 1$.

Unfortunately, the ceilings of throughput can be observed at high value of ρ_I. In similar way, Fig. 9 plots highest throughput corresponding to $\zeta = 0.01$. It can be seen that

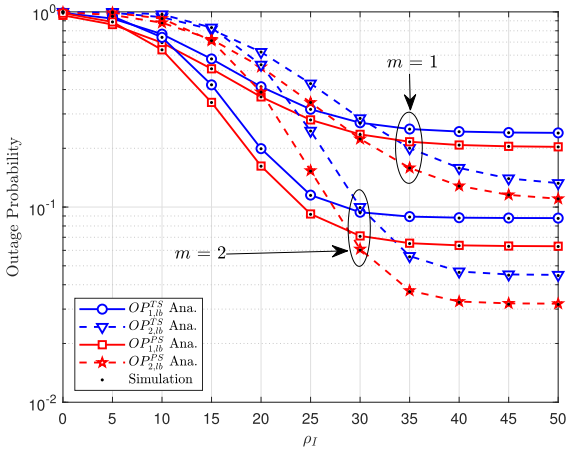

FIGURE 11. The outage probability versus transmit ρ_I with different values of m, where $\vartheta = 0.1$, $\delta = 0.1$, $\eta = 0.9$, $R_{th} = 1$ and $\zeta = 0.01$.

at serious situation of imperfect SIC, such overall throughput is very low, i.e. it equals to 0.2 at $\zeta = 0.5$. While $R_{th1} = 0.2$, $R_{th1} = 0.5$, $R_{th1} = 1$ are three cases of fixed target rates correspond to throughput as Fig. 10. The reason is that such throughput depends on both fixed target rates and achieved outage probability. In this case, outage performance is fixed by simulated parameters and throughput is mainly depend on the fixed target rates.

Unlike case of CR-NOMA over Rayleigh fading, the outage performance can be improved at $m = 2$ as Nakagami-m fading is considered as Fig. 11. Different with the Rayleigh distribution, one property of the Nakagami distribution is that the m parameter. We study how m can describe the fading severity of the propagation channel. In this study, we investigate the effect of channel fading on the performances of the CR-NOMA system by comparing the changes in the metrics two values of m parameters. It is confirmed correctness of our derived expressions.

VII. CONCLUSION

In this study, the system performance of the cooperative EH-assisted CR-NOMA is examined in term of outage probability and throughput. In particular, the closed-form expressions for outage probability are derived to evaluate performance of users in secondary network over both Rayleigh fading and Nakagami-m fading with interference constraint from primary network. The derived closed-form expressions were validated by numerical results, and the outage events of two users were compared in term of EH protocol, i.e. TS and PS. They provided slight varying performance as comparison between TS and PS. The proposed CR-NOMA showed best outage performance as reasonable selection of time switching/power splitting factors in EH protocol. Moreover, the numerical results showed that the proper selection of power allocation factors and EH parameters can guarantee the performance fairness for both users.

APPENDIX A

Recall the part of expected outage probability, Ξ_1 can be expressed as

$$\begin{aligned}\Xi_1 &= \Pr\left\{|h_{SR}|^2 > \theta_2^{TS}|h_{SP}|^2, |h_{SR}|^2 \right.\\ &\quad \left. > \gamma_{th1}^{TS}\bar{\alpha}|g_{SR}|^2 + \theta_1^{TS}|h_{SP}|^2\right\}\\ &= \Pr\left\{|h_{SR}|^2 > \theta^{TS}|h_{SP}|^2, |g_{SR}|^2 \right.\\ &\quad \left. < \frac{|h_{SR}|^2 - \theta_1^{TS}|h_{SP}|^2}{\gamma_{th1}^{TS}\bar{\alpha}}\right\} \end{aligned} \tag{73}$$

Then, Ξ_1 can be determined by

$$\begin{aligned}\Xi_1 &= \int_0^\infty f_{|h_{SP}|^2}(x)\bar{F}_{|h_{SR}|^2}\left(\theta^{TS}x\right)dx\\ &\quad - \int_0^\infty f_{|h_{SP}|^2}(x)\int_{\theta^{TS}x}^\infty f_{|h_{SR}|^2}(y)\,\bar{F}_{|g_{SR}|^2}\left(\frac{y-\theta_1^{TS}x}{\gamma_{th1}^{TS}\bar{\alpha}}\right)dydx.\end{aligned} \tag{74}$$

With the help of (17) and (18), $\bar{F}_{h_j}(x) = 1 - F_{h_j}(x)$ and after some mathematical transformation, we can simplify Ξ_1 as

$$\Xi_1 = \mathcal{J}_1^{TS} - \frac{\mathcal{J}_2^{TS}\lambda_{SR}}{\mathcal{J}_3^{TS}\lambda_{SP} + \lambda_{SR}}. \tag{75}$$

It completes the proof.

APPENDIX B

From the corresponding definition, we have term Ξ_2 as in (76), as shown at the bottom of the next page.

In which $Z = \frac{|h_{SR}|^2}{|h_{SP}|^2}$ and $\chi = \frac{2\eta\delta}{(1-\delta)}$. Then, we denote A_1 and A_2 are the first and second term of (76), respectively. In particular, A_1 is computed by

$$\begin{aligned}A_1 &= \int_0^\infty f_Z(z)\int_{\frac{1}{z\chi}}^\infty f_{|h_{RP}|^2}(y)F_{|h_1|^2}\left(\theta^{TS}y\right)dydz\\ &\quad - \int_0^\infty f_Z(z)\int_{\frac{1}{z\chi}}^\infty f_{|h_{RP}|^2}(y)\int_{\theta^{TS}y}^\infty f_{|h_1|^2}(x)\\ &\quad \times\bar{F}_{|g_1|^2}\left(\frac{x-\theta_1^{TS}y}{\gamma_{th1}^{TS}\bar{\alpha}}\right)dxdydz,\end{aligned} \tag{77}$$

and A_1 is rewritten as

$$\begin{aligned}A_1 &= \mathcal{Q}_1^{TS}\int_0^\infty f_Z(z)e^{-\frac{\theta^{TS}\lambda_{RP}+\lambda_1}{\chi\lambda_1\lambda_{RP}z}}dz\\ &\quad - \frac{\mathcal{J}_2^{TS}\lambda_1}{\mathcal{J}_3^{TS}\lambda_{RP}+\lambda_1}\int_0^\infty f_Z(z)e^{-\frac{\mathcal{J}_3^{TS}\lambda_{RP}+\lambda_1}{\chi\lambda_1\lambda_{RP}z}}dz,\end{aligned} \tag{78}$$

where $\mathcal{Q}_1^m = \frac{\lambda_1}{\theta^m\lambda_{RP}+\lambda_1}$ and $\mathcal{Q}_2^m = \frac{\lambda_2}{\theta_2^m\lambda_{RP}+\lambda_2}$. Moreover, the PDF of Z is given by [41]

$$f_Z(z) = \frac{\lambda_{SR}\lambda_{SP}}{(\lambda_{SP}z+\lambda_{SR})^2}. \tag{79}$$

Next, we substituting $t = \frac{\lambda_{SR}}{(t-\lambda_{SP})}$ in (78) and A_1 can rewritten as

$$A_1 = \mathcal{Q}_1^{TS}\lambda_{SP}e^{\theta^{TS}\wp_1^{TS}+\mathcal{C}^{TS}}\int_{\lambda_{SP}}^{\infty}\frac{e^{-\frac{\theta\lambda_{RP}+\lambda_1}{\chi\lambda_1\lambda_{RP}\lambda_{SR}}t}}{t^2}dz$$
$$-\frac{\mathcal{J}_2^{TS}\lambda_1\lambda_{SP}e^{\mathcal{J}_3^{TS}\wp_1^{TS}+\mathcal{C}^{TS}}}{\mathcal{J}_3^{TS}\lambda_{RP}+\lambda_1}\int_{\lambda_{SP}}^{\infty}\frac{e^{-\frac{\mathcal{J}_3^{TS}\lambda_{RP}+\lambda_1}{\chi\lambda_1\lambda_{RP}\lambda_{SR}}t}}{t^2}dz. \tag{80}$$

Further, based on [42, 3.471] the closed-form expression of A_1 is formulated as (23).

Then, A_2 is formulated as in (81). Similarly, A_2 is calculated as (24).

$$A_2 = \int_0^{\infty} f_Z(z)\bar{F}_{|h_1|^2}\left(\frac{\theta}{Z\chi}\right)dz$$
$$-\int_0^{\infty} f_Z(z)\bar{F}_{|h_1|^2}\left(\frac{\theta}{Z\chi}\right)\bar{F}_{|h_{RP}|^2}\left(\frac{1}{\chi Z}\right)dz$$
$$-\int_0^{\infty} f_Z(z)\int_{\frac{\theta}{Z\chi}}^{\infty} f_{|h_1|^2}(x)\bar{F}_{|g_1|^2}\left(\frac{Zx-\frac{\theta_1^{TS}}{\chi}}{\gamma_{th1}^{TS}\bar{\alpha}Z}\right)dxdz$$
$$+\int_0^{\infty} f_Z(z)\int_{\frac{\theta}{Z\chi}}^{\infty} f_{|h_1|^2}(x)\bar{F}_{|g_1|^2}\left(\frac{Zx-\frac{\theta_1^{TS}}{\chi}}{\gamma_{th1}^{TS}\bar{\alpha}Z}\right)$$
$$\times\bar{F}_{|h_{RP}|^2}\left(\frac{1}{\chi Z}\right)dxdz \tag{81}$$

Substituting (23) and (24) into (76), it leads to the final expected formula.

It is the end of the proof.

APPENDIX C

First, we denote the first and second term of (73) are P_1 and P_2 respectively. Then, based on (41), (42) and [42, 3.351.3], P_1 can be expressed as

$$P_1 = \int_0^{\infty} f_{|h_{SP}|^2}(x)\bar{F}_{|h_{SR}|^2}\left(\theta^{TS}x\right)dx$$
$$= \sum_{i=0}^{m_{SR}-1}\left(\frac{\theta}{\Omega_{SR}}\right)^i\frac{1}{i!\Gamma(m_{SP})\Omega_{SP}^{m_{SP}}}$$
$$\times\int_0^{\infty} x^{m_{SP}+i-1}e^{-\left(\frac{1}{\Omega_{SP}}+\frac{\theta^{TS}}{\Omega_{SR}}\right)x}dx$$
$$= \sum_{i=0}^{m_{SR}-1}\binom{m_{SP}+i-1}{m_{SP}-1}\frac{\bar{\Omega}^{m_{SP}}\left(\theta^{TS}\right)^i}{\left(\bar{\Omega}+\theta^{TS}\right)^{m_{SP}+i}}, \tag{82}$$

where $\bar{\Omega} = \frac{\Omega_{SR}}{\Omega_{SP}}$. Next, relying on [42, 1.111] P_2 can be further expressed by

$$P_2 = \int_0^{\infty} f_{|h_{SP}|^2}(x)\int_{\theta^{TS}x}^{\infty} f_{|h_{SR}|^2}(y)\bar{F}_{|g_{SR}|^2}\left(\frac{y-\theta_1^{TS}x}{\gamma_{th1}^{TS}\bar{\alpha}}\right)dydx$$
$$= \sum_{i=0}^{m_{SR}-1}\sum_{p=0}^{i}\binom{i}{p}\frac{(-1)^p\left(\theta_1^{TS}\right)^p}{i!\left(\Omega_{SR}\zeta^{TS}\right)^i}$$
$$\times\int_0^{\infty} f_{|h_{SP}|^2}(x)x^p e^{\frac{\theta_1^{TS}x}{\Omega_{SR}\zeta^{TS}}}dx$$
$$\times\int_{\theta^{TS}x}^{\infty} f_{|h_{SR}|^2}(y)y^{i-p}e^{-\frac{y}{\Omega_{SR}\zeta^{TS}}}dy. \tag{83}$$

Following result from [42, Eq. 3.351.2] and after some simple manipulations, A_2 can be obtained as

$$P_2 = \sum_{i=0}^{m_{SR}-1}\sum_{p=0}^{i}\sum_{k=0}^{m_{SR}+i-p-1}\binom{m_{SR}+i-p-1}{m_{SR}-1}$$
$$\times\frac{\Gamma(m_{SP}+p+k)!}{p!k!\Gamma(m_{SP})\left(1+\zeta^{TS}\right)^{m_{SR}+i-p-k}}$$

$$\Xi_2 = \Pr\left(\frac{\alpha_2\rho_I|h_1|^2}{\alpha_1\rho_I|h_1|^2+|h_{RP}|^2(\varepsilon+1)} > \gamma_{th2}^{TS}, \frac{\alpha_1\rho_I|h_1|^2}{\alpha_2\rho_I|g_1|^2+|h_{RP}|^2(\varepsilon+1)} > \gamma_{th1}^{TS}, \chi\rho_I Z > \frac{\rho_I}{|h_{RP}|^2}\right)$$
$$+\Pr\left(\frac{\alpha_2\chi\rho_I Z|h_1|^2}{\alpha_1\chi\rho_I Z|h_1|^2+(\varepsilon+1)} > \gamma_{th2}^{TS}, \frac{\alpha_1\chi\rho_I Z|h_1|^2}{\alpha_2\chi\rho_I Z|g_1|^2+(\varepsilon+1)} > \gamma_{th1}^{TS}, \chi\rho_I Z < \frac{\rho_I}{|h_{RP}|^2}\right)$$
$$= \Pr\left(|h_1|^2 > \theta^{TS}|h_{RP}|^2, |g_1|^2 < \frac{|h_1|^2-\theta_1^{TS}|h_{RP}|^2}{\gamma_{th1}^{TS}\bar{\alpha}}, |h_{RP}|^2 > \frac{1}{\chi Z}\right)$$
$$+\Pr\left(|h_1|^2 Z > \frac{\theta^{TS}}{\chi}, |g_1|^2 < \frac{Z|h_1|^2-\frac{\theta_1^{TS}}{\chi}}{\gamma_{th1}^{TS}\bar{\alpha}Z}, |h_{RP}|^2 < \frac{1}{\chi Z}\right). \tag{76}$$

$$B_2 = \underbrace{\int_0^\infty f_{Z_{-1}}(z)\bar{F}_{|h_1|^2}\left(\frac{\theta z}{\chi}\right)dz}_{B_{2,1}} - \underbrace{\int_0^\infty f_{Z_{-1}}(z)\bar{F}_{|h_1|^2}\left(\frac{\theta z}{\chi}\right)\bar{F}_{|h_{RP}|^2}\left(\frac{z}{\chi}\right)dz}_{B_{2,2}}.$$
$$- \underbrace{\int_0^\infty f_{Z_{-1}}(z)\int_{\frac{\theta z}{\chi}}^\infty f_{|h_1|^2}(x)\bar{F}_{|g_1|^2}\left(\frac{x-\theta_1^{TS}z\chi^{-1}}{\gamma_{th1}^{TS}\bar{\alpha}}\right)dxdz}_{B_{2,3}} + \underbrace{\int_0^\infty f_{Z_{-1}}(z)\int_{\frac{\theta z}{\chi}}^\infty f_{|h_1|^2}(x)\bar{F}_{|h_{RP}|^2}\left(\frac{z}{\chi}\right)\bar{F}_{|g_1|^2}\left(\frac{x-\theta_1^{TS}z\chi^{-1}}{\gamma_{th1}^{TS}\bar{\alpha}}\right)dxdz}_{B_{2,4}}. \quad (89)$$

$$\times\frac{(-1)^p\left(\theta_1^{TS}\right)^p\left(\theta^{TS}\right)^k\left(\zeta^{TS}\right)^{m_{SR}+m_{SP}}\bar{\Omega}^{m_{SP}}}{\left(\bar{\Omega}\zeta_1^{TS}-\theta_1^{TS}+\theta^{TS}+\zeta^{TS}\theta^{TS}\right)^{m_{SP}+p+k}}. \quad (84)$$

With the help of (82) and (84), we can obtain (44) This complete the proof.

APPENDIX D

Based on (76), in this case we denote the first term is B_1. Then, B_1 can be simplified in (85)

$$B_1 = \underbrace{\int_0^\infty f_{Z^{-1}}(z)\int_{\frac{z}{\chi}}^\infty f_{|h_{RP}|^2}(y)\bar{F}_{|h_1|^2}\left(\theta^{TS}y\right)}_{B_{1,1}}$$
$$- \underbrace{\int_0^\infty f_{Z^{-1}}(z)\int_{\frac{z}{\chi}}^\infty f_{|h_{RP}|^2}(y)\int_{\theta^{TS}y}^\infty f_{|h_1|^2}(x)\bar{F}_{|g_1|^2}\left(\frac{x-\theta_1^{TS}y}{\gamma_{th1}^{TS}\bar{\alpha}}\right)}_{B_{1,2}}. \quad (85)$$

Similar, $B_{1,1}$ can be further shown as

$$B_{1,1} = \sum_{i=0}^{m_1-1}\frac{1}{i!\Gamma(m_{RP})\Omega_{RP}^{m_{RP}}}\left(\frac{\theta^{TS}}{\Omega_1}\right)^i \times\int_0^\infty f_{Z^{-1}}(z)\int_{\frac{z}{\chi}}^\infty y^{m_{RP}+i-1}e^{-\left(\frac{1}{\Omega_{RP}}+\frac{\theta^{TS}}{\Omega_1}\right)y}dydz. \quad (86)$$

Based on [42, 3.351.2], it can be further shown $B_{1,1}$ as

$$B_{1,1} = \sum_{i=0}^{m_1-1}\sum_{p=0}^{m_{RP}+i-1}\binom{m_{RP}+i-1}{m_{RP}-1} \times\frac{(I_1)^{m_{RP}-p}}{p!(\Omega_{RP}\chi)^p(I_1+1)^{m_{RP}+i-p}} \times\int_0^\infty f_{Z^{-1}}(z)z^p e^{-\left(\frac{1}{\Omega_{RP}}+\frac{\theta^{TS}}{\Omega_1}\right)\frac{z}{\chi}}dz, \quad (87)$$

where $I_1 = \frac{\Omega_1}{\Omega_{RP}\theta^{TS}}$. Moreover, with the help of (45) in Lemma 1, and hence $B_{1,1}$ is rewritten by

$$B_{1,1} = \sum_{i=0}^{m_1-1}\sum_{p=0}^{m_{RP}+i-1}\binom{m_{RP}+i-1}{m_{RP}-1} \times\frac{(I_1)^{m_{RP}-p}\Upsilon(m_{SR}+m_{SP})}{p!\Upsilon\bar{\Omega}^{m_{SR}}(\Omega_{RP}\chi)^p(I_1+1)^{m_{RP}+i-p}} \times\int_0^\infty\frac{z^{m_{SP}+p-1}}{\left(\bar{\Omega}^{-1}+z\right)^{m_{SR}+m_{SP}}}e^{-\left(\frac{1}{\Omega_{RP}}+\frac{\theta^{TS}}{\Omega_1}\right)\frac{z}{\chi}}dz. \quad (88)$$

Substituting (46) into (88) and after some algebraic manipulations, $B_{1,1}$ is given as (49). Similarly, after some variable substitutions and manipulations, we can be achieve $B_{1,2}$ as (50).

Moreover, it can be computed B_2 as in the second term of (10) as in (89), as shown at the top of this page.

Then, $B_{2,1}$ is expressed as (51). Similarly, we can formulate $B_{2,2}$ as (52). Next, $B_{2,3}$ can be written by (53). Then, $B_{2,4}$ is given by (54).

Finally with results from (51), (52), (53) and (54), we can obtain (89) and the proof is completed.

REFERENCES

[1] S. M. R. Islam, N. Avazov, O. A. Dobre, and K.-S. Kwak, "Power-domain non-orthogonal multiple access (NOMA) in 5G systems: Potentials and challenges," *IEEE Commun. Surveys Tuts.*, vol. 19, no. 2, pp. 721–742, 2nd Quart., 2017.

[2] M. Elbayoumi, M. Kamel, W. Hamouda, and A. Youssef, "NOMA-assisted machine-type communications in UDN: State-of-the-Art and challenges," *IEEE Commun. Surveys Tuts.*, early access, Mar. 3, 2020, doi: 10.1109/COMST.2020.2977845.

[3] D.-T. Do, M. Vaezi, and T.-L. Nguyen, "Wireless powered cooperative relaying using NOMA with imperfect CSI," in *Proc. IEEE Globecom Workshops (GC Wkshps)*, Dec. 2018, pp. 1–6.

[4] D. Wan, M. Wen, F. Ji, H. Yu, and F. Chen, "On the achievable sum-rate of NOMA-based diamond relay networks," *IEEE Trans. Veh. Technol.*, vol. 68, no. 2, pp. 1472–1486, Feb. 2019.

[5] D.-T. Do and M.-S. Van Nguyen, "Device-to-device transmission modes in NOMA network with and without wireless power transfer," *Comput. Commun.*, vol. 139, pp. 67–77, May 2019.

[6] X. Li, Q. Wang, H. Peng, H. Zhang, D.-T. Do, K. M. Rabie, R. Kharel, and C. C. Cavalcante, "A unified framework for HS-UAV NOMA networks: Performance analysis and location optimization," *IEEE Access*, vol. 8, pp. 13329–13340, 2020.

[7] X. Li, M. Liu, C. Deng, D. Zhang, X.-C. Gao, K. M. Rabie, and R. Kharel, "Joint effects of residual hardware impairments and channel estimation errors on SWIPT assisted cooperative NOMA networks," *IEEE Access*, vol. 7, pp. 135499–135513, 2019.
[8] Y. Liu, Z. Qin, M. Elkashlan, Z. Ding, A. Nallanathan, and L. Hanzo, "Non-orthogonal multiple access for 5G and beyond," 2018, *arXiv:1808.00277*. [Online]. Available: http://arxiv.org/abs/1808.00277
[9] J. Men, J. Ge, and C. Zhang, "Performance analysis for downlink relaying aided non-orthogonal multiple access networks with imperfect CSI over nakagami-*m* fading," *IEEE Access*, vol. 5, pp. 998–1004, 2017.
[10] F. Zhou, Y. Wu, R. Q. Hu, Y. Wang, and K. K. Wong, "Energy-efficient NOMA enabled heterogeneous cloud radio access networks," *IEEE Netw.*, vol. 32, no. 2, pp. 152–160, Mar. 2018.
[11] Q. Li, M. Wen, E. Basar, H. V. Poor, and F. Chen, "Spatial modulation-aided cooperative NOMA: Performance analysis and comparative study," *IEEE J. Sel. Topics Signal Process.*, vol. 13, no. 3, pp. 715–728, Jun. 2019.
[12] J. Wang, Q. Peng, Y. Huang, H.-M. Wang, and X. You, "Convexity of weighted sum rate maximization in NOMA systems," *IEEE Signal Process. Lett.*, vol. 24, no. 9, pp. 1323–1327, Sep. 2017.
[13] Q. N. Le, D.-T. Do, and B. An, "Secure wireless powered relaying networks: Energy harvesting policies and performance analysis," *Int. J. Commun. Syst.*, vol. 30, no. 18, p. e3369, Dec. 2017.
[14] F. Zhou, Z. Li, N. C. Beaulieuz, J. Cheng, and Y. Wang, "Resource allocation in wideband cognitive radio with SWIPT: Max-min fairness guarantees," in *Proc. IEEE Global Commun. Conf. (GLOBECOM)*, Dec. 2016, pp. 1–6.
[15] Q. Wu, M. Tao, D. W. Kwan Ng, W. Chen, and R. Schober, "Energy-efficient resource allocation for wireless powered communication networks," *IEEE Trans. Wireless Commun.*, vol. 15, no. 3, pp. 2312–2327, Mar. 2016.
[16] F. Fang, H. Zhang, J. Cheng, and V. C. M. Leung, "Energy-efficient resource allocation for downlink non-orthogonal multiple access network," *IEEE Trans. Commun.*, vol. 64, no. 9, pp. 3722–3732, Sep. 2016.
[17] R. Zhang and C. K. Ho, "MIMO broadcasting for simultaneous wireless information and power transfer," *IEEE Trans. Wireless Commun.*, vol. 12, no. 5, pp. 1989–2001, May 2013.
[18] Y. Chen, N. Zhao, and M.-S. Alouini, "Wireless energy harvesting using signals from multiple fading channels," *IEEE Trans. Commun.*, vol. 65, no. 11, pp. 5027–5039, Nov. 2017.
[19] I. Krikidis, "Relay selection in wireless powered cooperative networks with energy storage," *IEEE J. Sel. Areas Commun.*, vol. 33, no. 12, pp. 2596–2610, Dec. 2015.
[20] X.-X. Nguyen and D.-T. Do, "Optimal power allocation and throughput performance of full-duplex DF relaying networks with wireless power transfer-aware channel," *EURASIP J. Wireless Commun. Netw.*, vol. 2017, no. 1, p. 152, Dec. 2017.
[21] I. Krikidis, T. Charalambous, and J. S. Thompson, "Stability analysis and power optimization for energy harvesting cooperative networks," *IEEE Signal Process. Lett.*, vol. 19, no. 1, pp. 20–23, Jan. 2012.
[22] I. Krikidis, "Average age of information in wireless powered sensor networks," *IEEE Wireless Commun. Lett.*, vol. 8, no. 2, pp. 628–631, Apr. 2019.
[23] D.-T. Do and H.-S. Nguyen, "A tractable approach to analyzing the energy-aware two-way relaying networks in the presence of co-channel interference," *EURASIP J. Wireless Commun. Netw.*, vol. 2016, no. 1, Dec. 2016.
[24] S. Arzykulov, G. Nauryzbayev, T. A. Tsiftsis, and B. Maham, "Performance analysis of underlay cognitive radio nonorthogonal multiple access networks," *IEEE Trans. Veh. Technol.*, vol. 68, no. 9, pp. 9318–9322, Sep. 2019.
[25] L. Bariah, S. Muhaidat, and A. Al-Dweik, "Error performance of NOMA-based cognitive radio networks with partial relay selection and interference power constraints," *IEEE Trans. Commun.*, vol. 68, no. 2, pp. 765–777, Feb. 2020.
[26] Y. Liu, Z. Ding, M. Elkashlan, and J. Yuan, "Nonorthogonal multiple access in large-scale underlay cognitive radio networks," *IEEE Trans. Veh. Technol.*, vol. 65, no. 12, pp. 10152–10157, Dec. 2016.
[27] R. Sun, Y. Wang, X. Wang, and Y. Zhang, "Transceiver design for cooperative non-orthogonal multiple access systems with wireless energy transfer," *IET Commun.*, vol. 10, no. 15, pp. 1947–1955, Oct. 2016.
[28] Y. Liu, Z. Ding, M. Elkashlan, and H. V. Poor, "Cooperative non-orthogonal multiple access with simultaneous wireless information and power transfer," *IEEE J. Sel. Areas Commun.*, vol. 34, no. 4, pp. 938–953, Apr. 2016.
[29] Y. Zhang and J. Ge, "Impact analysis for user pairing on NOMA-based energy harvesting relaying networks with imperfect CSI," *IET Commun.*, vol. 12, no. 13, pp. 1609–1614, Aug. 2018.
[30] M. Ashraf, A. Shahid, J. W. Jang, and K.-G. Lee, "Energy harvesting non-orthogonal multiple access system with multi-antenna relay and base station," *IEEE Access*, vol. 5, pp. 17660–17670, 2017.
[31] Y. Xu, C. Shen, Z. Ding, X. Sun, S. Yan, G. Zhu, and Z. Zhong, "Joint beamforming and power-splitting control in downlink cooperative SWIPT NOMA systems," *IEEE Trans. Signal Process.*, vol. 65, no. 18, pp. 4874–4886, Sep. 2017.
[32] L. Lv, J. Chen, Q. Ni, and Z. Ding, "Design of cooperative non-orthogonal multicast cognitive multiple access for 5G systems: User scheduling and performance analysis," *IEEE Trans. Commun.*, vol. 65, no. 6, pp. 2641–2656, Jun. 2017.
[33] Y. Chen, L. Wang, and B. Jiao, "Cooperative multicast non-orthogonal multiple access in cognitive radio," in *Proc. IEEE Int. Conf. Commun. (ICC)*, Paris, France, May 2017, pp. 1–6.
[34] S. Arzykulov, T. A. Tsiftsis, G. Nauryzbayev, and M. Abdallah, "Outage performance of cooperative underlay CR-NOMA with imperfect CSI," *IEEE Commun. Lett.*, vol. 23, no. 1, pp. 176–179, Jan. 2019.
[35] G. Im and J. H. Lee, "Outage probability for cooperative NOMA systems with imperfect SIC in cognitive radio networks," *IEEE Commun. Lett.*, vol. 23, no. 4, pp. 692–695, Apr. 2019.
[36] B. Li, X. Qi, K. Huang, Z. Fei, F. Zhou, and R. Q. Hu, "Security-reliability tradeoff analysis for cooperative NOMA in cognitive radio networks," *IEEE Trans. Commun.*, vol. 67, no. 1, pp. 83–96, Jan. 2019.
[37] D. Wang and S. Men, "Secure energy efficiency for NOMA based cognitive radio networks with nonlinear energy harvesting," *IEEE Access*, vol. 6, pp. 62707–62716, 2018.
[38] W. Liang, K. D. Wang, J. Shi, L. Li, and G. K. Karagiannidis, "Distributed sequential coalition formation algorithm for spectrum allocation in underlay cognitive radio networks," *IEEE Access*, vol. 7, pp. 56803–56816, 2019.
[39] G. Nauryzbayev, S. Arzykulov, T. A. Tsiftsis, and M. Abdallah, "Performance of cooperative underlay CR-NOMA networks over Nakagami-m channels," in *Proc. IEEE Int. Conf. Commun. Workshops (ICC Workshops)*, May 2018, pp. 1–6.
[40] Y. Yu, Z. Yang, Y. Wu, J. A. Hussein, W.-K. Jia, and Z. Dong, "Outage performance of NOMA in cooperative cognitive radio networks with SWIPT," *IEEE Access*, vol. 7, pp. 117308–117317, 2019.
[41] A. Papoulis, *Probability, Random Variables, and Stochastic Processes*, 4th ed. New York, NY, USA: McGraw-Hill, 2002.
[42] I. S. Gradshteyn and I. M. Ryzhik, *Table of Integrals, Series, and Products*, 6th ed. San Diego, CA, USA: Academic, 2000.

DINH-THUAN DO (Senior Member, IEEE) received the B.S., M.Eng., and Ph.D. degrees in communications engineering from Vietnam National University (VNU-HCMC), in 2003, 2007, and 2013, respectively. He was a Visiting Ph.D. Student with the Communications Engineering Institute, National Tsing Hua University, Taiwan, from 2009 to 2010. Prior to joining Ton Duc Thang University, he was a Senior Engineer at the VinaPhone Mobile Network, from 2003 to 2009. He published one book and one book chapter. He has authored or coauthored over 120 technical articles published in peer-reviewed international journals (ISI/Scopus) and over 60 conference papers. His research interests include signal processing in wireless communications networks, MIMO, NOMA, UAV networks, satellite systems, physical layer security, device-to-device transmission, and energy harvesting. He was a recipient of the Golden Globe Award from Vietnam Ministry of Science and Technology (Top 10 Talent Young Scientist in Vietnam), in 2015. He received the Creative Young Medal, in 2015. He was a lead guest editor in several special issues in peer-reviewed journals. He serves as an Associate Editor in seven ISI/Scopus journals.

ANH-TU LE was born in Lam Dong, Vietnam, in 1997. He is currently pursuing the master's degree in communication and information system fin field of wireless communication. He is currently a Research Assistant with the WICOM Lab, which was led by Dr. Thuan. He has authored or coauthored over five technical articles published in peer-reviewed international journals. His research interests include the wireless channel modeling, NOMA, cognitive radio, and MIMO.

BYUNG MOO LEE (Member, IEEE) received the Ph.D. degree in electrical and computer engineering from the University of California at Irvine, CA, USA, in 2006.

He is currently an Associate Professor at the School of Intelligent Mechatronics Engineering, Sejong University, Seoul, South Korea. Prior to joining Sejong University, he had ten years of industry experience, including research positions at the Samsung Electronics Seoul Research and Development Center, Samsung Advanced Institute of Technology, and Korea Telecom Research and Development Center. During his industry experience, he participated in the IEEE 802.16/11, Wi-Fi Alliance, and 3GPP LTE standardizations, and also participated in Mobile VCE and Green Touch Research Consortiums, where he made numerous contributions and filed a number of related patents. His research interests are in the areas of wireless communications, signal processing, and machine learning applications. He served as the Vice Chairman of the Wi-Fi Alliance Display MTG, from 2015 to 2016.